Under-Ice Phytoplankton Blooms: Shedding Light on the "Invisible" Part of Arctic Primary Production

Mathieu Ardyna, C. Mundy, Nicolas Mayot, Lisa Matthes, Laurent Oziel, Christopher Horvat, Eva Leu, Philipp Assmy, Victoria Hill, Patricia A Matrai, et al.

frontiers in Marine Science

REVIEW
published: 19 November 2020
doi: 10.3389/fmars.2020.608032

Under-Ice Phytoplankton Blooms: Shedding Light on the "Invisible" Part of Arctic Primary Production

Mathieu Ardyna[1,2], C. J. Mundy[3], Nicolas Mayot[4,5], Lisa C. Matthes[3], Laurent Oziel[2,6,7], Christopher Horvat[8], Eva Leu[9], Philipp Assmy[10], Victoria Hill[11], Patricia A. Matrai[4], Matthew Gale[3,12], Igor A. Melnikov[13] and Kevin R. Arrigo[1]*

[1] Department of Earth System Science, Stanford University, Stanford, CA, United States, [2] Sorbonne Université, CNRS, Laboratoire d'Océanographie de Villefranche, LOV, Paris, France, [3] Centre for Earth Observation Science, Clayton H. Riddell Faculty of Environment, Earth, and Resources, University of Manitoba, Winnipeg, MB, Canada, [4] Bigelow Laboratory for Ocean Sciences, East Boothbay, ME, United States, [5] School of Environmental Sciences, Faculty of Science, University of East Anglia, Norwich, United Kingdom, [6] Takuvik Joint International Laboratory, Laval University (Canada)—CNRS (France), UMI3376, Département de Biologie et Québec-Océan, Université Laval, Québec, QC, Canada, [7] Alfred Wegener Institute for Polar and Marine Research, Bremerhaven, Germany, [8] Institute at Brown for Environment and Society, Brown University, Providence, RI, United States, [9] Akvaplan-niva, CIENS, Oslo, Norway, [10] Norwegian Polar Institute, Fram Centre, Tromsø, Norway, [11] Department of Ocean, Earth, and Atmospheric Science, College of Sciences, Old Dominion University, Norfolk, VA, United States, [12] Environmental Health Program, Health Canada, Winnipeg, MB, Canada, [13] P.P. Shirshov Institute of Oceanology (RAS), Moscow, Russia*

OPEN ACCESS

Edited by:
Paul F. J. Wassmann, Arctic University of Norway, Norway

Reviewed by:
Klaus Martin Meiners, Australian Antarctic Division, Australia
Mar Fernández-Méndez, GEOMAR Helmholtz Center for Ocean Research Kiel, Germany

***Correspondence:**
Mathieu Ardyna
ardyna@stanford.edu

Specialty section:
This article was submitted to Global Change and the Future Ocean, a section of the journal Frontiers in Marine Science

Received: *18 September 2020*
Accepted: *26 October 2020*
Published: *19 November 2020*

Citation:
Ardyna M, Mundy CJ, Mayot N, Matthes LC, Oziel L, Horvat C, Leu E, Assmy P, Hill V, Matrai PA, Gale M, Melnikov IA and Arrigo KR (2020) Under-Ice Phytoplankton Blooms: Shedding Light on the "Invisible" Part of Arctic Primary Production. Front. Mar. Sci. 7:608032. doi: 10.3389/fmars.2020.608032

The growth of phytoplankton at high latitudes was generally thought to begin in open waters of the marginal ice zone once the highly reflective sea ice retreats in spring, solar elevation increases, and surface waters become stratified by the addition of sea-ice melt water. In fact, virtually all recent large-scale estimates of primary production in the Arctic Ocean (AO) assume that phytoplankton production in the water column under sea ice is negligible. However, over the past two decades, an emerging literature showing significant under-ice phytoplankton production on a pan-Arctic scale has challenged our paradigms of Arctic phytoplankton ecology and phenology. This evidence, which builds on previous, but scarce reports, requires the Arctic scientific community to change its perception of traditional AO phenology and urgently revise it. In particular, it is essential to better comprehend, on small and large scales, the changing and variable icescapes, the under-ice light field and biogeochemical cycles during the transition from sea-ice covered to ice-free Arctic waters. Here, we provide a baseline of our current knowledge of under-ice blooms (UIBs), by defining their ecology and their environmental setting, but also their regional peculiarities (in terms of occurrence, magnitude, and assemblages), which is shaped by a complex AO. To this end, a multidisciplinary approach, i.e., combining expeditions and modern autonomous technologies, satellite, and modeling analyses, has been used to provide an overview of this pan-Arctic phenological feature, which will become increasingly important in future marine Arctic biogeochemical cycles.

Keywords: under-ice phytoplankton blooms, biogeochemical cycles, nutrient, sea ice, climate change, Arctic Ocean

HISTORICAL PERSPECTIVE: UNDER-ICE BLOOMS, AN OVERLOOKED PHENOLOGICAL FEATURE

The idea of phytoplankton blooms developing underneath an ice cover, also called under-ice blooms (UIBs), had been sporadically reported in the past (see below) but became widely accepted by the scientific community only after a massive UIB was reported in the Chukchi Sea (Arrigo et al., 2012, 2014). The hypothesis that light inhibits the development of phytoplankton blooms under a snow, ice, and ice algal cover had previously prevailed in the Arctic scientific community's thinking. This assumption has likely led to significant errors in estimates of Arctic-wide production and phytoplankton phenology. For example, it was suggested that net primary production over Arctic shelves could be up to an order of magnitude larger than currently estimated from open water measurements (Arrigo et al., 2012). However, the assumption is not new. In fact, studies in the early part of the last century concluded that thick ice and low temperatures limited the development of phytoplankton under the central Arctic ice pack (Nansen, 1902; Gran, 1904; Sverdrup, 1929).

Noted by English (1961), it was Braarud (1935) who first put forward the idea that, although limited by light, phytoplankton can still grow under the Arctic pack ice. It was suggested that the use of phytoplankton nets with relatively coarse mesh size at the time may have missed the abundant but smaller sized fraction of the phytoplankton community. Confirming the hypothesis of under-ice phytoplankton production, Shirshov (1944) showed that a seasonal cycle of phytoplankton development occurred northeast of Greenland under the 3 m thick permanent ice pack with maximum chlorophyll *a* (Chl *a*) concentrations reaching 0.4 mg m^{-3} in the upper 20 m of the water column. Again, one of the limitations of this work was the use of nets to collect phytoplankton samples, the tool available at the time.

It was not until two decades later, during the 1957–58 International Geophysical Year (IGY) drift station expeditions, that the opportunity arose to observe annual cycles of phytoplankton standing stocks and production using the more modern techniques of the time. The end result of this work was nothing less than an incredible first glimpse of UIBs occurring in the central Arctic (Apollonio, 1959; English, 1961). Both studies demonstrated the progression of what we term "classical" UIBs, where bloom development begins slowly under a melting snow cover and fully develops under melt pond-covered sea ice. Unfortunately, both of these papers have remained in relative obscurity, the first having been published as a short note in the *IGY Bulletin* (Apollonio, 1959), and the second as a scientific report (English, 1961). In other words, both research papers are difficult to access using today's online search engines, which limited their use in the flourish of papers on UIBs over the last decade. It is for this purpose that we include key data from these studies in **Figure 1** to showcase their relevant observations.

The two separate drift stations, Alpha and Bravo, drifting on opposite sides of the Beaufort High Gyre, showed surprisingly similar results (**Figure 1**). Both sites had a 3 m thick multiyear ice cover with hummocks reaching more than 9 m thick and ∼1% lead coverage (estimates by aircraft; Apollonio, 1959; English, 1961). At both sites, the observed UIBs were initiated during the snowmelt period in July after the solstice insolation peak and quickly ended when snow began to accumulate. This prevailing light limitation driven by the snow cover is particularly evident when comparing the 1957 and 1958 UIBs at Alpha station. A longer snow-free period during summer led to a longer lasting UIB. It is impossible to quantitatively compare integrated Chl *a* values between these years due to inconsistencies in sampling depths (**Figure 1A**). Melt ponds started to form during the first week of July at Alpha station in both 1957 and 1958, covering 15–30% of the ice pack surface. This melt pond coverage closely matches more recent reports for multiyear ice ranging from 6.8 to 25% (Fetterer and Untersteiner, 1998; Nicolaus et al., 2012; Huang et al., 2016). Of course, the most dramatic change is the loss of multiyear ice (MYI) and its replacement by first-ice year ice (FYI) and the resulting increase in light transmission during the melt period (Nicolaus et al., 2012; Horvat et al., 2017).

A comparison between Alpha and Bravo stations in 1957 suggests that production of phytoplankton biomass was greater at Alpha station, where the maximum Chl *a* concentration was >1.5 mg m^{-3} (**Figure 1A**; English, 1961) *versus* at Bravo station where it was only 0.37 mg Chl *a* m^{-3} just under the ice (Apollonio, 1959). Furthermore, while the integrated Chl *a* biomass was estimated over a depth interval of 100 m at Bravo station, the maximum biomass was only ∼21 mg m^{-2} versus the >30 mg Chl *a* m^{-2} estimated at Alpha station and only integrated over the upper 20 m. Similarly, averaged daily production, directly estimated by ^{14}C incubation at Bravo station, was about half that of a more conservative estimate derived from the net Chl *a* accumulation rate at the Alpha station (**Table 1**). The central Arctic ice pack tends to be more convergent along the northern edge of the Canadian Archipelago (Haas et al., 2017). It is likely that drift station Bravo had more deformed (hummock) ice with a thicker ice cover and hence greater light limitation that would help to explain the observed lower Chl *a* concentrations. Both studies concluded that light limitation controlled under-ice primary production. In fact, English (1961) conducted a nutrient addition experiment and found no response, suggesting that nutrients were not limiting. However, Apollonio (1959) concluded that although light availability controlled phytoplankton production, the nitrogen-depleted upper 150 m water column, with NO_3:PO_4 ratios averaging 7:1 relative to the Redfield ratio of 16:1 (Redfield et al., 1963), would ultimately constrain the central Arctic to have one of the lowest productivities in the world even if light limitation was not a prime factor.

Since those early studies, UIBs in the Arctic have received a modest amount of attention based on the number of times those features have been described in the literature (**Table 1** and **Figure 2**). Additional datasets from online and unpublished data sources confirm the occurrence of UIBs. **Table 1** shows that after the IGY studies, there was a period of more than three decades before direct documentation of UIBs were published (e.g., Michel et al., 1993, 1996; Strass and Nöthig, 1996; Gosselin et al., 1997). However, it is clear that UIBs were occurring during this gap of published literature. In fact, UIBs were observed in the early 1960s in Jones Sound (Apollonio and Matrai, 2011) and from the mid-1980s to the 1990s near Resolute

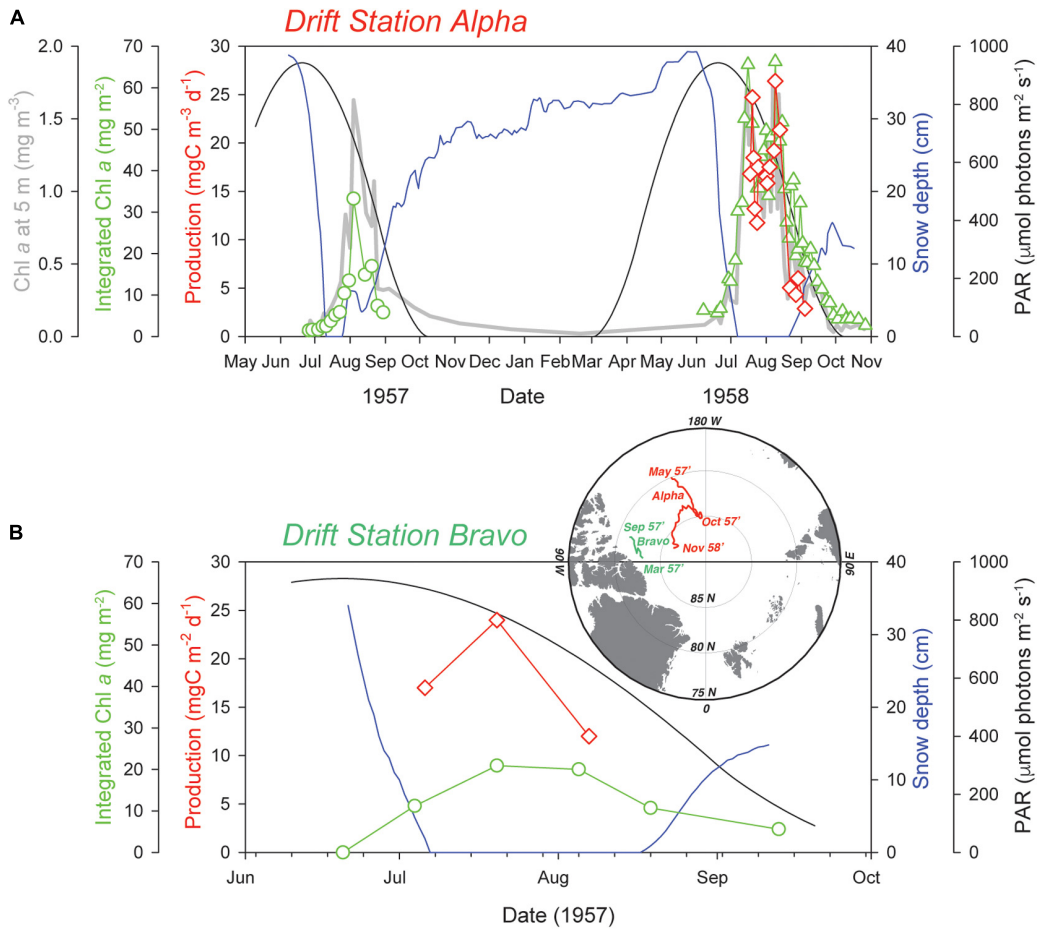

FIGURE 1 | Historic (1957–58) UIBs in the Central Arctic Ocean. Time series of top of the atmosphere photosynthetically active radiation (PAR) for 83°N latitude, as well as snow depth, primary production and chlorophyll *a* concentration estimates during the 1957–58 International Geophysical Year (IGY) at Drift station Alpha (English, 1961; **A**) and Drift station Bravo (Apollonio, 1959; **B**). Primary production estimates were derived from 6 m water samples incubated for 6–12 h at 200 foot candles (~4 µmol photons m^{-2} s^{-1}) at Drift station Alpha (English, 1961) and via *in situ* bottle incubations for 24 h at Drift station Bravo (Apollonio, 1959), both studies using ^{14}C tracer incubations. Data were extracted from figures in the respective publications using the shareware program DataThief III.

Bay in the Canadian Arctic Archipelago (**Table 1**). Reports of UIBs after the mid-1990s remained relatively sporadic (e.g., Yager et al., 2001; Fortier et al., 2002; Mundy et al., 2009; Leu et al., 2011) until the last decade when the occurrence of UIBs was documented for almost all Arctic and sub-Arctic marine regions (**Table 1**). The recent effort to improve our understanding of UIBs has led to dedicated scientific programs [e.g., Arctic-ICE (Mundy et al., 2014), FAABulous (Leu et al., pers. comm.), Green Edge (Oziel et al., 2019; Randelhoff et al., 2019), ICESCAPE (Arrigo et al., 2012), N-ICE (Assmy et al., 2017), SUBICE (Arrigo et al., 2017)] as well as the deployment of new monitoring technologies (Laney et al., 2014; Hill et al., 2018; Mayot et al., 2018; Boles et al., 2020; Randelhoff et al., 2020) and directed modeling efforts (e.g., Palmer et al., 2014; Zhang et al., 2015; Horvat et al., 2017; Lowry et al., 2018; Kinney et al., 2020). In this paper, we attempt to provide the state of the art of our knowledge of UIBs, by focusing on their ecology and environmental control, but also their regional specificities (in terms of occurrence, magnitude, and assemblages), which are shaped by the complexity of the rapidly changing Arctic physico-chemical environment. To this end, a multidisciplinary approach, i.e., combining expeditions and modern autonomous technologies (see "Box 1: New technologies: More insights on under-ice biogeochemical cycles and blooms"), satellite, and modeling analyses, has been used to provide an overview of this pan-Arctic phenological feature, which should become increasingly important in future Arctic biogeochemical cycles.

CHANGING UNDER-ICE LIGHT REGIME, PRECURSOR TO UNDER-ICE BLOOMS?

Large-Scale Under Sea-Ice Light Regimes

As a consequence of a warming Arctic climate, Arctic sea ice melts earlier and more widely, leading to Arctic-wide reductions in sea-ice thickness and age (Kwok, 2018; Stroeve and Notz, 2018).

TABLE 1 | Summary table of Pan-Arctic UIBs.

Location	Year	UI maximum daily production (g C m^{-2} d^{-1})	UI average daily production (g C m^{-2} d^{-1})	UI maximum chlorophyll *a* (mg m^{-3})	UI maximum integrated chlorophyll *a* (mg m^{-2})	Integration depth (m)	Latitude (°N)	Longitude (°)	References
Central Arctic									
Ice Station Bravo	1957	0.024	0.018	0.37	21	>100	83	−100	Apollonio, 1959
Ice Station Alpha	1957		0.032**	1.6	33	20	83	−155	English, 1961
	1958		0.12**	1.8	66.3	4-64	83	−165	English, 1961
	1994	0.073	0.03		26	Euphotic depth	83 (76–90)	−180	Gosselin et al., 1997
	2011			0.6	12	50	78.00	−130.00	Laney et al., 2014
	2017			0.5	11	50	84.50	7.00	Boles et al., 2020
	2017			1.48	57	100	82.50	10.00	Boles et al., 2020
Chukchi Sea									
	1998			19	392	50	72.15	−161.65	Yager et al., 2001
	2011	3.7		77	1290	60	73.17	−168.49	Arrigo et al., 2012, 2014
	2014		0.083**	8.8	91	5–20	71.57	−153.07	Hill et al., 2018
Canadian High Arctic									
Amundsen Gulf	2008		1.4*	25	345	50	69.83	−123.63	Mundy et al., 2009
Cambridge Bay	2014		0.013*	0.9	14.8	40	69.03	−105.33	Mundy, unpublished
	2018		0.029*	0.82	22	40	69.11	−105.06	Back et al., 2020
Resolute Passage/Barrow Strait	1984		0.4**	8.9	194	50	74.62	−94.82	Codispoti et al., 2013
	1985			14.5	255	50	74.62	−94.82	Codispoti et al., 2013
	1986		0.59**	21.7	302	50	74.62	−94.82	Codispoti et al., 2013
	1986		0.68**	22.9	344	50	74.67	−94.9	Devine et al., 2014
	1987			9.1	239	50	74.67	−94.9	Devine et al., 2014
	1990			11.9	234	40	74.62	−94.82	Codispoti et al., 2013
	1991			6.2	148	50	74.62	−94.82	Codispoti et al., 2013
	1992			51	166	15	74.69	−95.27	Michel et al., 1996; Fortier et al., 2002
	1994		0.86**		455	90	74.75	−95.83	Fortier et al., 2002
	1995		0.55**		383	90	74.43	−97.16	Fortier et al., 2002
	2010		1.1*	15.4	508	50	74.71	−95.25	Mundy et al., 2014
	2011		1.2*	11.1	310	40	74.72	−95.15	Galindo et al., 2014
Jones Sound	1961	1.97		10.5	76.2	10	75.72	−84.5	Apollonio and Matrai, 2011
	1962	1.63		10.3	124	15	75.72	−84.5	Apollonio and Matrai, 2011
	1963	1.16		11.8	138	15	75.72	−84.5	Apollonio and Matrai, 2011

(Continued)

TABLE 1 | Continued

Location	Year	UI maximum daily production (g C m^{-2} d^{-1})	UI average daily production (g C m^{-2} d^{-1})	UI maximum chlorophyll *a* (mg m^{-3})	UI maximum integrated chlorophyll *a* (mg m^{-2})	Integration depth (m)	Latitude (°N)	Longitude (°)	References
Baffin Bay	2015	0.050	0.0121	8.64	152	60	67.48	−63.79	Oziel et al., 2019
	2016	0.739	0.1251	5.12	182	60	67.48	−63.79	Oziel et al., 2019
Greenland Sea									
	2012/14		0.31*	2.4	87	70	73.50	−15.00	Mayot et al., 2018
Barents Sea									
	1991			3.5	131	50	77.5	33.0	Strass and Nöthig, 1996
North of Svalbard									
	2015		0.57*	7.5	233	50	80.886	8.537	Assmy et al., 2017

Summary of maximum and average carbon production and chlorophyll concentration estimates for under-ice blooms observed in the Arctic Ocean.

*Net community production estimated from integrated nitrate drawdown during UIB.

**Net accumulation rate estimated from time series of integrated chlorophyll concentrations during exponential bloom phase of UIB.

Arctic sea ice is now predominantly thin, first or second-year ice, and large areas formerly covered by sea ice year-round are now ice-free in summer (Kwok, 2018; Stroeve and Notz, 2018). Arctic warming also leads to an earlier transition from snow- to melt pond-covered ice, which significantly reduces the albedo of the ice-covered Arctic Ocean (AO) earlier in the year, and closer to peak insolation of the annual solar cycle (Perovich et al., 2007). Reduced surface albedo due to a greater melt pond coverage of FYI compared to MYI (Nicolaus et al., 2012; Perovich and Polashenski, 2012) and reduced attenuation by thinner ice are crucial for the initiation of UIBs (Arrigo et al., 2012, 2014; Oziel et al., 2019; Ardyna et al., 2020). Together, these factors lead to a substantial increase in the availability of photosynthetically active radiation (PAR; 400–700 nm) for primary production in the ice-covered upper ocean, making widespread UIBs a possibility that was hypothesized by Mundy et al. (2009) and recently recognized (Horvat et al., 2017; Kinney et al., 2020).

Due to the lack of long-term observations of the under-ice light field, climate model hindcasts can provide a useful tool for examining trends in light availability in the ice-covered Arctic surface layer. Here, we analyze the ensemble climate model statistics from 11 historical (1850–2014) CESM2 simulations submitted to CMIP6 for each month between June and August (panels from left to right; **Figure 3**). Note that the CICE5.1 model used in CESM2 employs a Delta-Eddington scheme for reflection, absorption, and transmission of solar radiation as a function of sea-ice thickness, surface type, and sea-ice inherent optical properties. This scheme has been extensively validated, accurately reproducing optical properties of Arctic sea ice (Briegleb and Light, 2007; Light et al., 2008). **Figures 3A–C** show the total extent of sea ice and the total extent of the compact ice zone (CIZ), defined as the total area where the concentration of sea ice is greater than 80%, and thus the area where there is sufficient sea ice for UIBs to be relevant. The modeled trend in the loss of CIZ extent reflects and exceeds the loss in total sea-ice extent, resulting in a larger fraction of the Arctic being covered with low concentration sea ice (a result found across CMIP6 models), and little sea ice in CESM2 is considered "compact" by August.

The remaining compact ice, however, is more transparent. The Arctic-average PAR flux (μmol photons m^{-2} s^{-1}) through sea ice in the CIZ has increased dramatically (**Figures 3D–F**), doubling in June and July, when the transitions in sea-ice surface type are most dramatic. These model results are consistent with recent observations by Castellani et al. (2020) who measured the highest daily integrated under-ice PAR levels (i.e., 4.46–20.71 mol photons m^{-2} d^{-1}) in the central Arctic in June–July. To estimate what fraction of the CIZ could support UIBs, we used a simple critical depth model (Sverdrup, 1953; and a threshold value for PAR flux of 34 μmol photons m^{-2} s^{-1} with a 20 m deep mixed layer; see Horvat et al. (2017) for the choice of all parameters used here). Up to 2.5 × 10^6 km^2 of the ice-covered AO permitted UIBs in June (**Figure 3G**), compared to 3.5 × 10^6 km^2 in July (**Figure 3H**), despite the declining area of the CIZ in July (**Figure 3B**). During this month, in up to 100% of the CIZ, under-ice PAR levels were above the threshold of 34 μmol photons m^{-2} s^{-1}, which allows for net

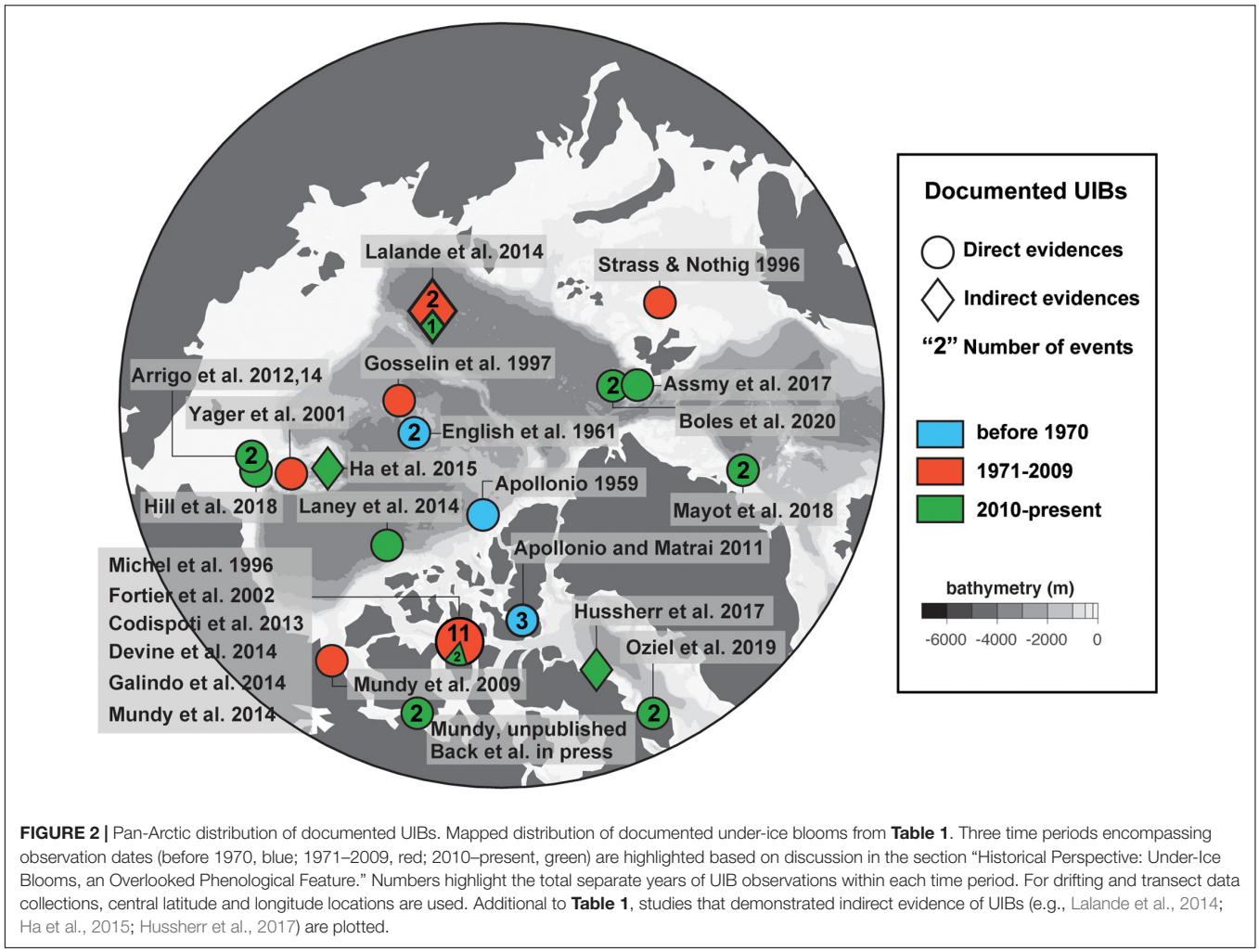

FIGURE 2 | Pan-Arctic distribution of documented UIBs. Mapped distribution of documented under-ice blooms from **Table 1**. Three time periods encompassing observation dates (before 1970, blue; 1971–2009, red; 2010–present, green) are highlighted based on discussion in the section "Historical Perspective: Under-Ice Blooms, an Overlooked Phenological Feature." Numbers highlight the total separate years of UIB observations within each time period. For drifting and transect data collections, central latitude and longitude locations are used. Additional to **Table 1**, studies that demonstrated indirect evidence of UIBs (e.g., Lalande et al., 2014; Ha et al., 2015; Hussherr et al., 2017) are plotted.

phytoplankton growth and biomass increase. Interestingly, large portions of the AO may have permitted UIBs in the surface layer in the past, amounting to about 2×10^6 km^2 in July or between 30 and 40% of CIZ area (10–20% of total sea-ice extent). This can help explain why sporadic UIBs were recorded in the past (see the section "Historical Perspective: Under-Ice Blooms, an Overlooked Phenological Feature"). That is, historical light conditions could occasionally be sufficient for UIBs to develop, though their frequency has likely greatly increased over the past several decades.

The geographical pattern of modeled light field changes for the months of June to August also provides some interesting insights (**Figure 4**). The 2010–2014 average ensemble mean downwelling PAR through sea ice demonstrates that the regions permitting UIBs are confined to the periphery of the CIZ in June, but extend over most of the Arctic in July. This is a recent change; historically during July (**Figure 4E**), the areas supporting UIBs lay outside of the modern CIZ, and UIBs were only found on the periphery of the (historical) July CIZ. The difference between these two areas is largely broad-based and non-regional, with the signature of larger changes in sea-ice thickness and melt state rather than the imprint of regional variability.

While the overall under-ice light availability increased with decreasing ice thickness over recent decades, small-scale sea-ice features such as the geometry of melt ponds at the ice surface, ridges, hummocks, leads, and the horizontal distribution of light absorbing ice impurities cause spatial heterogeneity in PAR transmission (Ehn et al., 2008, 2011; Light et al., 2008; Frey et al., 2011; Katlein et al., 2014, 2016; Matthes et al., 2019; Horvat et al., 2020). The resulting complexity of the under-ice light field creates difficulties in measuring and estimating light availability for UIB phytoplankton since algal cells drifting in under-ice surface waters are exposed to large variations in PAR throughout the day. Overlooking the complexity of the under-ice light field and its characteristic optical parameters can oversimplify model development and our general understanding of UIB phenology.

Small-Scale Heterogeneity in Light Propagation Through Arctic Sea Ice

After the return of the sun in spring, transmission of PAR through refrozen leads in the dynamic ice cover can trigger early season phytoplankton blooms beneath the still snow-covered sea ice (Assmy et al., 2017). Later, during melt pond formation,

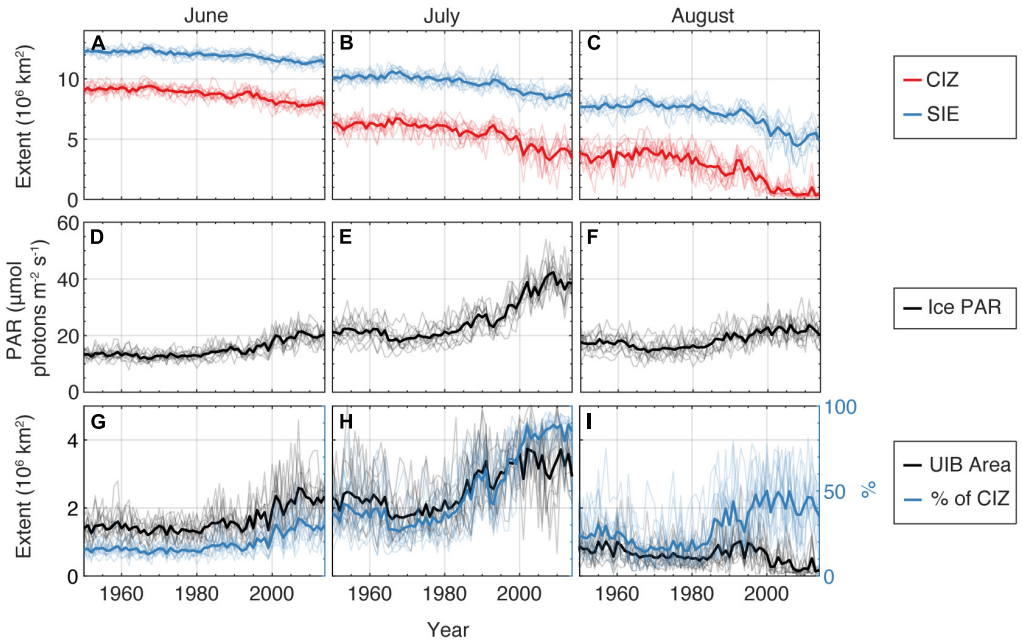

FIGURE 3 | Modeled arctic-wide properties of under-ice light from CESM2. **(A–C)** Arctic sea ice extent (blue) and compact ice zone (red) for months June–August for the 11 CESM2 contributions to CMIP6. Ensemble mean value is bold line, individual ensemble members thin lines. **(D–F)** Average PAR flux through sea ice in compact ice areas. **(G–I)** Area of regions supporting light-limited UIBs to 20 m depth (black, left axis), and (blue, right axis) fraction of compact ice zone permitting such UIBs.

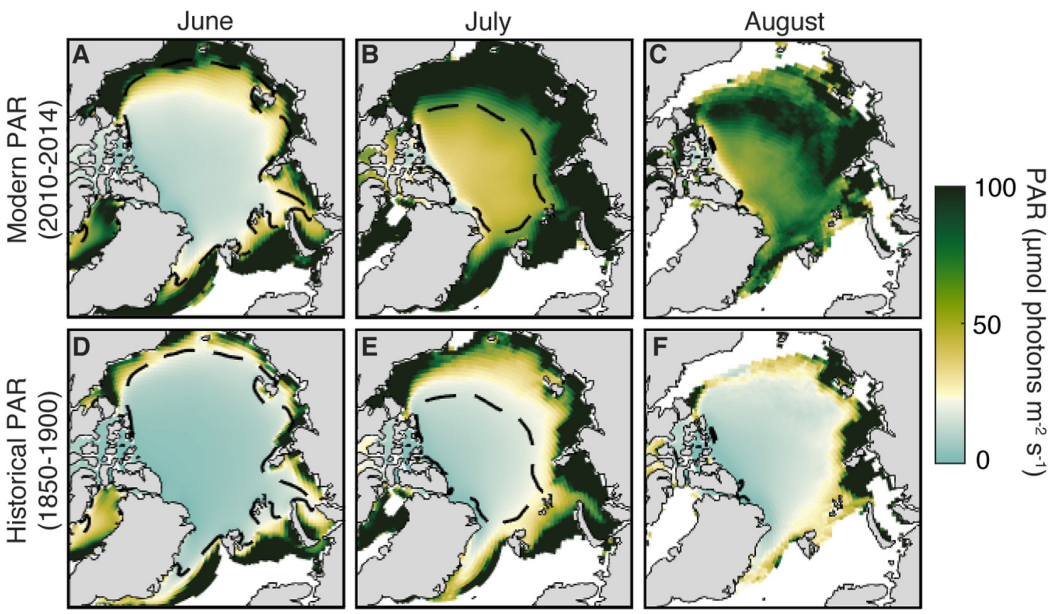

FIGURE 4 | Geography of modeled light transmission through Arctic sea ice. **(A–C)** Ensemble-mean average PAR flux through sea ice for the modern (2010–2014) period from June to August. The white point of the colormap is the threshold value for initiating an UIB (i.e., 34 µmol photons m^{-2} s^{-1}) and used in **Figures 3G–I**. **(D–F)** Same, but for the historical period (1850–1900). Dashed contour is the modern ensemble mean compact ice zone contour in each month. The present-day CIZ contour is given as a black dashed line.

regional PAR transmission through FYI increases rapidly to 25–31% (**Figure 5**, Katlein et al., 2019; Matthes et al., 2020), which marks the potential onset of an UIB and, simultaneously, the termination of the ice algal bloom (Oziel et al., 2019). Earlier bottom ablation and termination of the ice algal bloom also improves the under-ice light climate for phytoplankton and can

contribute to the initiation of UIBs (Mundy et al., 2014). Another key prerequisite for the initiation of an UIB is stratification of the surface layer induced by melt water addition (Oziel et al., 2019) as already suggested by Legendre et al. (1981).

As the euphotic zone starts to deepen until enhanced light attenuation by blooming phytoplankton reverses this process (**Figure 5**, Oziel et al., 2019), the increasing difference in light transmittance through ponded *versus* bare ice, combined with the lateral spreading of photons within the ice layer, create large fluctuations of up to 43% in under-ice PAR levels for drifting phytoplankton communities in the upper ocean beneath landfast sea ice (Matthes et al., 2020). Higher light transmission through more transparent nearby structures (i.e., refrozen leads, melt ponds, and bare ice) impacts the vertical radiation transfer in the water column causing edge effects at the ice bottom and subsurface irradiance maxima beneath bare ice adjacent to melt ponds (Ehn et al., 2011; Frey et al., 2011; Katlein et al., 2016).

During the melt season, the under-ice light field can change over a relatively short time and, in turn, can cause a large error in regional estimates of under-ice PAR availability for marine primary production. Single-location transmittance measurements beneath one ice surface type may not be representative of the average PAR experienced by phytoplankton cells that drift at a different rate and direction relative to the overlying sea ice. Perovich (2005) was the first to define the spatial scale of the minimal variation in the partitioning of incident solar radiation as an "aggregate scale". Using this approach, regional light transmission can be calculated as the sum of average transmission values for each surface type (melt ponds, bare ice, open water) multiplied by its areal fraction (e.g., Taskjelle et al., 2017; Katlein et al., 2019; Massicotte et al., 2019; Matthes et al., 2020).

Figure 5 highlights the complexity of the radiation field beneath the ice cover that creates large variations in the apparent optical properties, such as the diffuse vertical attenuation coefficient (K_d) and the average cosine coefficient (μ_d) of downwelling irradiance, which are used to calculate the depth of the euphotic zone and thereby the accessibility to subsurface inorganic nutrients for primary production. Subsurface maxima in PAR from higher light transmission through adjacent melt pond-covered ice alter the vertical light distribution, resulting in a non-exponential decrease in PAR with depth and difficulties

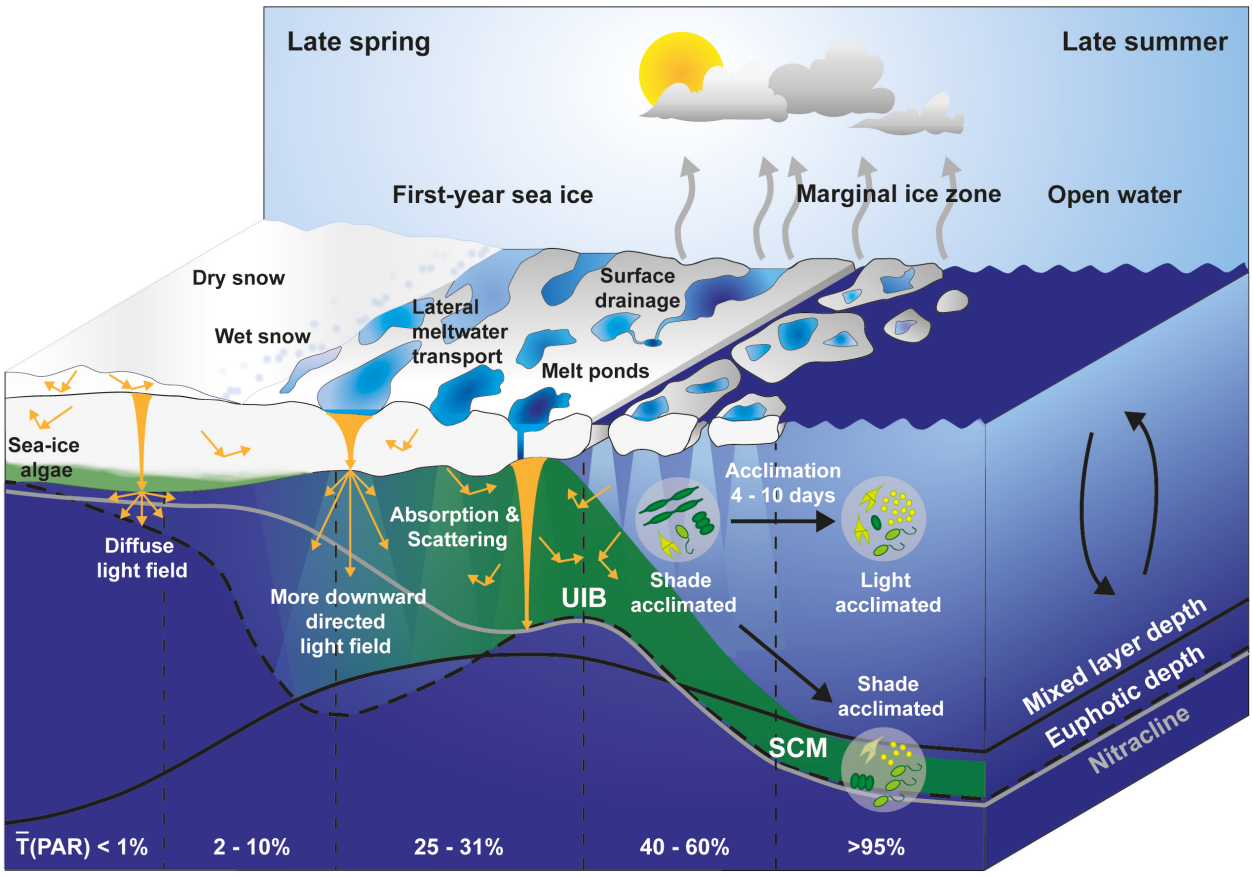

FIGURE 5 | Schematic of under-ice light field during the sea ice spring melt. Changes in the depth of the euphotic zone (black dashed line), mixed layer (black solid line), and nitracline (gray solid line) are presented in relation to the ice surface melt progression and the development of an under-ice bloom (UIB) and subsurface chlorophyll maximum (SCM) from late spring to late summer. Regional average transmission [$\bar{T}$(PAR)] at the water surface is provided for various sea ice surface types, marginal ice zone, and open water, respectively. State of photoacclimation is given for under-ice and open water phytoplankton communities.

in estimating K_d (Ehn et al., 2011; Frey et al., 2011; Katlein et al., 2016; Laney et al., 2017). Several studies investigated separation of the effects of water column attenuation from local spatial heterogeneity in transmittance through sea ice using semi-empirical models (Frey et al., 2011; Laney et al., 2017) or by deriving K_d from upwelling radiation (Massicotte et al., 2018). Besides a more robust K_d, the angular distribution of light in the surface water layer needs to be considered in the parametrization of the under-ice light field due to multiple scattering in the overlying snow and ice cover and/or enhanced backscattering of algal cells under bloom conditions (Ehn et al., 2011; Arrigo et al., 2014; Katlein et al., 2014; Pavlov et al., 2017). Considering this lateral photon transport, scalar radiometers with a spherical collector that capture PAR from all directions provide a more realistic measurement of light availability for primary production (Morel and Gentili, 2004; Pavlov et al., 2017; Matthes et al., 2019). If only downwelling planar PAR can be measured beneath the ice, a μ_d between 0.56 and 0.7 can be used to convert these measurements into downwelling scalar PAR (Arrigo et al., 1991, 2014; Ehn and Mundy, 2013; Katlein et al., 2014; Pavlov et al., 2017; Matthes et al., 2019).

Underestimating light availability in the ice-covered water column has large implications on the calculation of the euphotic zone (depths where PAR is >0.2–1% of surface PAR) or isolume (integrated daily irradiance of 0.4 mol photons m^{-2} d^{-1}, Letelier et al., 2004) depths and the investigation of the UIB onset. During pre-bloom conditions, light availability limits photosynthesis and under-ice phytoplankton communities are acclimated to low-light conditions. In this time period, the impact of errors in the under-ice light field parametrization on calculated primary production rates is largest due to the linear relationship between the rate of photosynthesis and increasing light levels before reaching saturation levels (Matthes et al., 2019).

Physiological Phytoplankton Assemblage Responses to Varying Light Regimes

Phytoplankton are well acclimated to the low-light under-ice environment by maximizing light absorption and photosynthetic capacity (Palmer et al., 2011, 2013; Lewis et al., 2019). As light transmission increases through melt pond formation and sea-ice melt, phytoplankton cells modify their pigment composition (Hill et al., 2005; Johnsen et al., 2018; Kauko et al., 2019), the number and size of their photosynthetic units (Matsuoka et al., 2009, 2011; Lewis et al., 2019) and through those adjustments change their measurable photosynthetic parameters of the photosynthetic machinery to maximize light utilization. Changes in the photoprotective to photosynthetic pigment ratio of under-ice phytoplankton communities to acclimate to the changing light availability have been observed as blooms progress. During pre-bloom and early bloom conditions, intracellular concentrations of Chl *a* and accessory pigments increase, supported by the abundant nutrients in the surface layer required for biosynthesis (Geider et al., 1998; Lewis et al., 2019). Although the high nutrient availability further supports large cell sizes, phytoplankton cells are heavily packed with pigments resulting in reduced cross sectional absorption (when absorption is normalized to pigment) due to self-shading (package effect; Morel and Bricaud, 1981; Hill et al., 2005; Matsuoka et al., 2011). Nevertheless, these pre-bloom communities are well adapted to achieve high rates of photosynthesis for small increases in under-ice light levels through a high photosynthetic efficiency, α, typical of low-light environments, paired with a high maximum rate of carbon fixation, P_{max} (Palmer et al., 2013; Lewis et al., 2019). Interestingly, the light saturation parameter, E_k, was found to be higher than the available average light intensity (Johnsen et al., 2018; Lewis et al., 2019). Lewis et al. (2019) concluded that under-ice phytoplankton communities are "primed" for later season increases in light availability. Hence, shade-acclimation allows algae to maximize their growth rate and to utilize the limited nutrient reservoir immediately once light levels increase through melt pond formation and ice melt. This acclimation strategy also enables phytoplankton to adjust quickly to the higher light conditions at ice edges (e.g., leads and polynyas; Palmer et al., 2011; Assmy et al., 2017; Lowry et al., 2018). In particular, pelagic diatoms were found to be able to rapidly acclimate successfully to drastically increased light conditions, in strong contrast to that of sea-ice diatoms (Kvernvik et al., 2020).

During bloom conditions at higher light intensities, under-ice communities increasingly synthesize photoprotective carotenoids (Hill et al., 2005; Joy-Warren et al., 2019; Kauko et al., 2019) and mycosporine-like amino acids (Elliott et al., 2015) that dissipate excess light energy as heat instead of channeling it to photosystems. This process of non-photochemical quenching enables a high degree of plasticity of the photosynthetic performance of bloom-forming species such as *Phaeocystis*, promoting its dominance under highly variable light regimes (Arrigo et al., 2010; Assmy et al., 2017; Joy-Warren et al., 2019). However, nitrate that is needed to synthesize proteins and pigments is often depleted during the late stage of an UIB, and thus impedes the photo-acclimation responses to increasing light levels by reducing the number of functional reaction centers and the photochemical efficiency of the photosynthetic machinery (Lewis et al., 2019, and citations therein). As shade-acclimated phytoplankton transition from a low-light regime beneath the ice into a high-light regime in open water, carbon fixation rates can decrease due to super-saturating light intensities (**Figure 5**, Palmer et al., 2011). According to the observations by Palmer et al. (2011), communities were able to acclimate to the high-light environment in the surface water after 4–10 days while phytoplankton at the subsurface chlorophyll maximum (SCM) remained shade-acclimated with comparable α and P_{max} to those of under-ice communities.

CONTRASTED REGIONAL ENVIRONMENTAL SETTINGS FAVORING UIBS

The AO is surrounded by land and has a complex topography of shelves, slopes, basins, channels, and sills. These features strongly constrain ocean circulation, primarily driven by both wind and buoyancy processes (Timmermans and Marshall, 2020)

and are influenced by the Atlantic and Pacific inflows. These warmer and saltier inflows are the main source of inorganic nutrients for the colder and fresher Arctic domain. Stratification is generally driven by salinity rather than temperature in the AO (*beta* rather than *alpha* oceans; *sensu* Carmack, 2007). Indeed, the AO generally acts as a freshwater reservoir especially in the anticyclonic Beaufort Gyre (Proshutinsky et al., 2019). Most (>50%) of this freshwater is received from rivers and, to a lesser extent, sea-ice melt and precipitation (Haine et al., 2015). Light availability above the sea-ice surface is dictated by the annual light cycle, which itself depends on latitude. However, the light transmitted to the ocean surface is controlled to a large extent by the properties of clouds (Bélanger et al., 2013), as well as sea ice and its overlying snow cover (see the section "Small-Scale Heterogeneity in Light Propagation Through Arctic Sea Ice").

The occurrence of UIBs, like open water phytoplankton blooms, is governed by bottom-up (e.g., temperature, light and nutrient availability, water column stability) and top-down (e.g., zooplankton grazing, viral infection, parasite infestation) controls. UIBs appear to be an ubiquitous feature of the Arctic spring bloom (see the section "Historical Perspective: Under-Ice Blooms, an Overlooked Phenological Feature"), but the mechanisms underlying their formation, as well as their phenology and species succession may be diverse due to regional specificities. Here we synthesize the currently available knowledge on the atmosphere-snow-ice-ocean processes that have been shown to control UIB dynamics. This approach enables both an assessment of the relevance of regional specificities (bathymetry, tides), as well as the influence of changing environmental conditions (i.e., sea ice, snow, ocean circulation, wind regimes) for future developments in UIB distribution and phenology (**Figures 6**, **7**).

Upwelling Systems

Wind-driven upwelling along the continental shelves, shelf breaks, and ice edges are a source of substantial change in water masses and cross-shelf transport (Williams and Carmack, 2015). They allow nutrient-rich subsurface water masses to shoal up to the surface over shelves. Such processes have been documented in several regions such as the Beaufort (Pickart et al., 2009; Jackson et al., 2015) and the Chukchi (Arrigo et al., 2014; Spall et al., 2014) seas. There, these upwelling systems are characterized by an eastward flowing Pacific shelf break jet overlying the offshore Atlantic boundary current (see **Figures 6A**, **7**).

The continental slope of the Beaufort Sea appears to present the most favorable upwelling conditions (Carmack and Chapman, 2003) for inducing UIBs because: (1) the shelf break is the shallowest and steepest of the AO (see **Figure 6A**; Randelhoff et al., 2018); (2) the region is characterized by persistent zonal wind regimes determined by the atmospheric circulation patterns of the Beaufort High and Aleutian Low; and (3) upwelling along the Canadian continental slope of the Beaufort Sea is favored by northeasterly wind regimes oriented along the bathymetric slope (Kirillov et al., 2016) and a westerly inversion of the normally eastward-flowing Pacific shelf break jet (Spall et al., 2014). Thus, when the wind regime allows it, nutrients are upwelled from the Beaufort basin at depth (typically winter Pacific or Atlantic waters; Schulze and Pickart, 2012; Pickart et al., 2013) and stimulate primary production on the Beaufort shelf (Carmack et al., 2004; Tremblay et al., 2011; Ardyna et al., 2017). On the Atlantic side, the presence of warm and nutrient-rich Atlantic waters at the surface in the region north and west of Svalbard during winter has been attributed to upwelling (Falk-Petersen et al., 2015), but later oceanographic campaigns have not found such evidence (Randelhoff et al., 2018). The occurrence of wind-driven upwelling in the European sector is rather unlikely because the area is not subject to upwelling-favorable winds (i.e., northeast winds) and the shelf slope is much deeper (Randelhoff and Sundfjord, 2018). By contrast, the Atlantic sector is much more sensitive to vertical mixing, wintertime convection and advection (Lind et al., 2018).

Advective Systems of the Atlantic Sector

The European sector is the most dynamic region of the AO, particularly along the Atlantic waterway which closely follows the slope of the Barents Sea continental shelf. At the very end of one of the branches of the Atlantic Current (i.e., the Svalbard branch), the Atlantic waters flow beneath the more buoyant polar surface waters, which are generally sea-ice covered until spring. This is a place where UIBs have been documented (**Figure 6B**) but the most important evidence of UIBs in this region was reported during the N-ICE expedition (Assmy et al., 2017). The authors suggested that Atlantic waters could play a second order role in seeding polar surface waters with phytoplankton cells from below and that light penetration through leads is likely to be the main environmental driver behind initiation of the UIB. Other studies have highlighted advective origins of UIBs in the region north of Svalbard (Johnsen et al., 2018). The ongoing "Atlantification" of the region is weakening the cold halocline and could favor the shoaling of nutrient-rich intermediate Atlantic waters (Polyakov et al., 2017).

Outflow Shelves

The Arctic outflow shelves are highly heterogeneous (Michel et al., 2015). Arctic sea ice advected over the East Greenland shelf extends offshore from the shelf break. Mayot et al. (2018) argued that UIBs in this offshore region are the result of local processes and may contribute up to 50% of annual primary production. These UIBs that occur in the Canadian Archipelago are typically driven by mixing (nutrient availability) processes and increased light availability during the spring ice melt (**Figure 6C**). The most recent studies collecting time series under landfast sea ice in the Canadian Archipelago (Resolute Bay: Mundy et al., 2014; Baffin Bay: Oziel et al., 2019) also concluded that the biomass was locally produced on these shelves. These sea ice camp studies helped resolve early temporal evolution of UIBs and revealed different key processes. Both the deepening of the euphotic zone due to increased light transmission and mixing/stratification processes acted together to trigger and drive UIB dynamics. Snow accumulation on landfast sea ice plays a critical role for UIB development by controlling most of the light transmitted to the under-ice water column (Mundy et al., 2014). In fact, light attenuation is strongly dominated by snow compared to sea ice. Extensive melt pond formation at the end

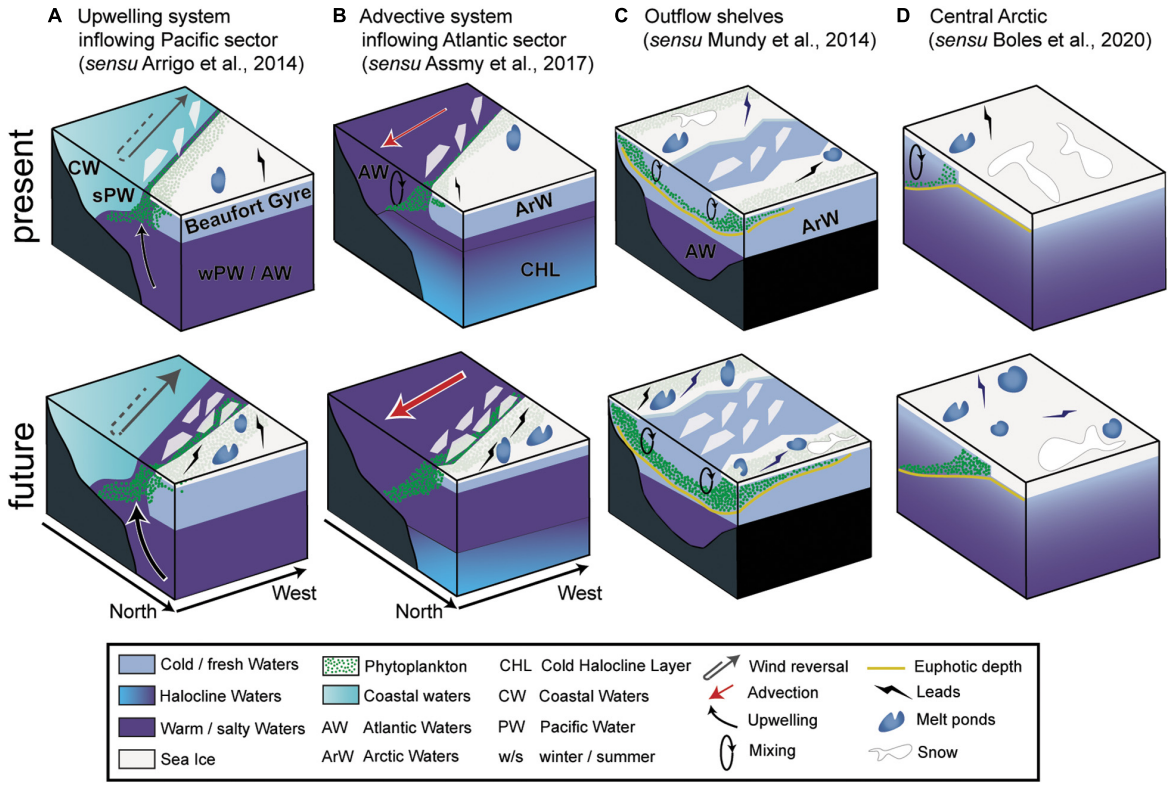

FIGURE 6 | Schematic drawing of the regional environmental settings favoring UIBs. The present and future different environmental settings for upwelling system inflowing **(A)** Pacific and **(B)** Atlantic sectors, **(C)** the outflow shelves, and **(D)** the Central Arctic. The atmospheric, sea-ice, and the water column compartments are shown.

of the snow melt period concomitant with the early stabilization of the upper water column due to freshwater input led to UIB initiation. As phytoplankton progressively consume nutrients in the surface layers, mixing is again of major importance to tap into deeper nutrient pools to maintain phytoplankton growth. In the Canadian Archipelago or Baffin Bay, tidal energy was the main source of vertical mixing (Mundy et al., 2014) that was enhanced by the presence of complex bathymetric features such as sills and shoals (Michel et al., 2006) or "Fjord-like" systems (Oziel et al., 2019). The tidal-induced mixing controlled the magnitude and depth of the SCM (Mundy et al., 2014; Oziel et al., 2019; Randelhoff et al., 2019).

The Central Arctic Ocean

Under-ice blooms in the central Arctic have been scarcely sampled but the recent shift from a MYI to a FYI-dominated sea-ice regime increases the likelihood of UIBs to occur there (Horvat et al., 2017; Kinney et al., 2020). The first *in situ* evidence of UIBs in the central Arctic under FYI was recently documented (Laney et al., 2014; Boles et al., 2020). Although significant relative to background Chl *a* levels, these UIBs were characterized by low biomass (i.e., ~0.5–1.4 mg Chl *a* m^{-3}), which was similar in magnitude to the UIBs documented under MYI in the central Arctic by Apollonio (1959) and English (1961) (**Table 1** and **Figure 1**). In these regions, surface layers are clearly both light and nutrient limited (**Figure 6D**). It is suggested that modal eddy-induced mixing could help sustain phytoplankton growth by providing nutrients from deeper Atlantic waters (Laney et al., 2014; Boles et al., 2020; Lewis et al., 2020).

DIVERSITY OF UNDER-ICE BLOOMS: PHENOLOGY, STRATEGY, ASSEMBLAGES

Origin and Initiation of UIBs

The initiation of an UIB requires a viable seed population of algal cells present in the euphotic zone of the water column under the ice. There are three potential seeding sources for UIBs: (a) algal cells in the water column, (b) vegetative cells or resting stages at the sediment surface, and (c) algal cells or resting stages entrapped in sea ice that are released during melt onset at the underside of the ice (Johnsen et al., 2020). Very little is known about the relative importance of these three different seeding strategies, but it likely varies strongly depending on mixing depth, bottom topography, and sea-ice conditions. In relatively shallow coastal areas, re-suspension of resting stages from sediment surfaces is considered to be an important source seeding the diatom component of the spring bloom (Hegseth et al., 2019). In deeper oceanic regions, however, pelagic and sea-ice melt

seeding by vegetative cells surviving the winter in the upper part of the water column are probably the most important seeding sources. Other important taxonomic groups of UIBs such as *Phaeocystis* are not known to form resting stages, but they have been found in single cell state throughout the winter in surface waters (Vader et al., 2015). While taxonomic composition and maximum biomass of an UIB seems to be strongly correlated with the type and amount of nutrients available (e.g., the winter nitrate:silicate ratio; Ardyna et al., 2020), the environmental cue for bloom initialization is an increase in light intensity, often caused by snow melt onset (Oziel et al., 2019; Ardyna et al., 2020) and sloughing of the ice algal community (Mundy et al., 2014).

Winters in high latitudinal areas are characterized by the Polar night when the sun does not rise above the horizon. This leads to extended periods where ambient irradiances are not sufficient for *in situ* primary production in ice-free surface waters (Kvernvik et al., 2018), and even less so underneath sea-ice cover (see also the previous section "Physiological Phytoplankton Assemblage Responses to Varying Light Regimes"). Phytoplankton have adapted through various strategies to cope with these conditions, ranging from mixotrophy/heterotrophy, resting stage formation, and utilization of internal lipid stores to survival of vegetative cells with lowered metabolic activity (Johnsen et al., 2020). Phytoplankton communities during wintertime are characterized by very low cell concentrations and a predominance of small, flagellated cells, as well as heterotrophic dinoflagellates (Lovejoy et al., 2007; Błachowiak-Samołyk et al., 2015; Brown et al., 2015; Vader et al., 2015). Among the small flagellated cells, two species that periodically dominate phytoplankton assemblages in Arctic waters were found throughout the Polar night: *Micromonas polaris* and *Phaeocystis pouchetii* (Vader et al., 2015). Natural microalgal assemblages, and in particular diatoms, are able to survive extended periods of darkness from months to years (Zhang et al., 1998; McMinn and Martin, 2013), while retaining their ability to resume physiological activity quickly once light returns (Kvernvik et al., 2018; Lacour et al., 2019; Morin et al., 2020). Diatoms also seem to retain their photophysiological characteristics during extended periods of darkness relatively unchanged as compared to flagellates, which possibly enables them to utilize the returning light in early spring very efficiently (van de Poll et al., 2020). Furthermore, mixotrophy (i.e., via osmotrophic or/and phagotrophic processes) also appears to be a widespread strategy among dinoflagellates and other photosynthetic flagellate taxa, keeping them active throughout the polar night (McMinn and Martin, 2013). However, important photosynthetic flagellates (e.g., green picoeukaryotes), such as *M. polaris*, are likely to rely on other strategies to survive through polar winter that have not yet been identified (Vader et al., 2015; Jimenez et al., 2020). This highlights the need for further study in the field.

Variability in UIB Biomass and Community Composition

Along the continental margins of the AO, UIBs are generally dominated by pelagic centric diatoms of the genera *Chaetoceros* and *Thalassiosira* and/or the colonial stage of the haptophyte alga *Phaeocystis*, with UIB magnitude decreasing and the role of *Phaeocystis* increasing toward the Atlantic sector (Ardyna et al., 2020). This overall pattern can be primarily attributed to the larger nutrient inventory and more upwelling-favorable conditions in the Pacific sector and the low silicate relative to nitrate concentrations in the Atlantic sector, respectively (Ardyna et al., 2020). A study from Darnley Bay in the Canadian Beaufort Sea showed that upwelling favorable conditions at the ice edge of landfast FYI in combination with the snow melt onset and low ice algal biomass throughout the study period provided both ample nutrients and light, including surface stratification, to fuel a large UIB (Mundy et al., 2009) dominated by the pennate diatom *Fragilariopsis oceanica* (Mundy et al., 2011). Furthermore, advection of high phytoplankton biomass produced in adjacent open water likely increased primary production capacity under the sea-ice cover (Mundy et al., 2009). Moderate UIBs (max. Chl *a* concentration of 4.3 mg m^{-3}), dominated initially by *Micromonas* sp. and diatoms and then by solitary (non-colonial) *Phaeocystis*, were observed in the Canadian Basin during the SHEBA ice camp in 1997/1998 (Sherr et al., 2003). A gradient in UIB biomass can be detected within the central AO, with the Amerasian Basins, particular the Beaufort Gyre, showing lower Chl *a* biomass than the Eurasian Basin (Laney et al., 2014) presumably due to the stronger haline stratification in the former. While light limitation in the central AO is progressively diminished by the shift from a MYI toward a FYI regime (Nicolaus et al., 2012; Horvat et al., 2017), the strong stratification limits nutrient input from below the halocline and will set an upper limit to UIB biomass accumulation. However, phytoplankton species are able to adapt their nutrient ratios, in addition to their photosynthetic parameters as discussed in the section "Physiological Phytoplankton Assemblage Responses to Varying Light Regimes," in response to variable *in situ* nutrient concentrations, as shown for Arctic phytoplankton in the Chukchi Sea (Mills et al., 2015).

A synthesis of observations (**Figure 8**) contrasts algal composition and succession associated with the distinct regional environmental conditions described in the section "Contrasted Regional Environmental Settings Favoring UIBs." Two expeditions were representative of the inflowing shelves describing the upwelling system in the Pacific sector (ICESCAPE cruise 2011 in the Chukchi Sea; **Figures 8B,D**) and the advective system in the Atlantic sector (N-ICE2015, north of Svalbard; **Figure 8A**). The other two expeditions were representative of the outflow shelves (i.e., the Canadian Arctic Archipelago, Resolute Passage 2010 and 2011; **Figure 8C**) and the central AO (North Pole expedition 2015; **Figure 8E**). All studies were conducted during the last decade, are thus representative of the new FYI regime, and cover the spring and summer season. One caveat common to these studies is that they were not following a Lagrangian design, i.e., following processes in the same water mass over time, but phytoplankton compositional patterns are still representative of the pre-bloom (except ICESCAPE) and bloom conditions. The N-ICE and North Pole expeditions in 2015 are representative of ice camps on drifting sea ice during the early spring to summer season while the Resolute Passage studies in 2010 and 2011 are representative of ice camps on landfast

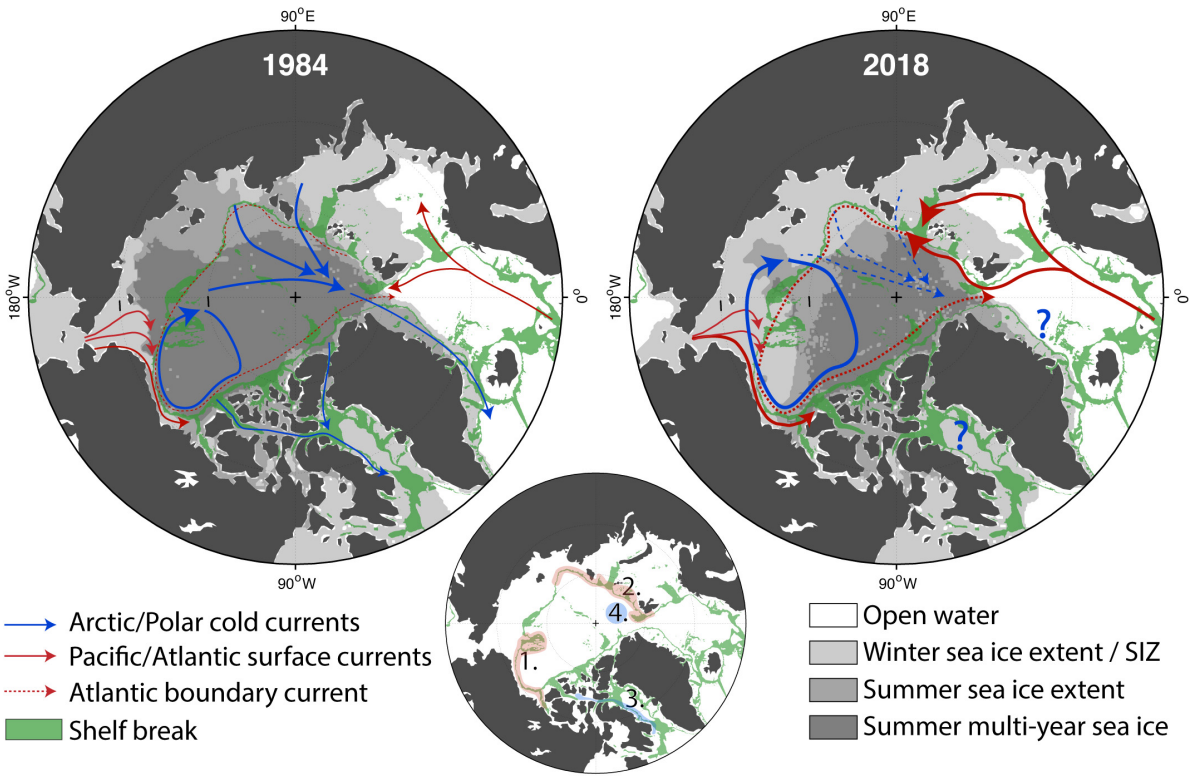

FIGURE 7 | Maps of the changes that occurred from 1984 to 2018 in sea ice and surface circulation versus unchanging geographic features (i.e., bathymetry). The green shading illustrates the shelf break (depth between 350 and 1200 m). The thinner the green band, the steeper the shelf break is. Dark gray: multiyear ice, medium gray: summer sea ice extent, light gray: winter sea ice extent, white: open ocean. The modern Seasonal Ice Zone (SIZ) is delimited by the winter sea ice extent and the summer sea ice extent which corresponds to the light gray area. Warm and salty currents carrying Pacific and Atlantic waters poleward are in red. Currents associated with fresher and colder Arctic waters are in blue. The UIBs case scenarios **(A)** and **(B)** are inflowing shelf systems (red), **(C)** is an outflowing shelf system (blue), and **(D)** corresponds to the central Arctic basins (from **Figure 6**). They are localized in the bottom panel. Note that the absence of MYI in the Canadian Archipelago is due to a land-influence limitation on the "age of sea ice" dataset (Tschudi et al., 2019).

ice covering the late spring to summer season. The ICESCAPE cruise in 2011 is based on oceanographic transects from open to ice-covered waters in the Chukchi Sea during the month of July. The ice camp studies provide information on phytoplankton community composition prior to the UIB peak while information from ICESCAPE is limited to the peak of the UIB.

All UIBs were dominated by diatoms with the exception of the N-ICE UIB which was dominated by *P. pouchetii* (Assmy et al., 2017; **Figure 9**). There is a gradual decrease in maximum phytoplankton bloom abundance from the shallower and more nutrient-rich Chukchi Sea and Resolute Passage toward the Atlantic sector and the central AO (**Figure 9**). Particularly, the central AO shows nearly two orders of magnitude lower peak abundances (**Figure 9**) as was also the case for AO production estimates and Chl *a* concentrations (**Table 1**). One common feature of all studies is that pennate diatoms and dinoflagellates dominated in the early phase of the UIB development. In particular *Fragilariopsis* and *Pseudo-nitzschia* species, but also other pennate diatoms commonly found in sea ice were prominent during the pre-bloom phase. Interestingly, pennate diatoms (*Fragilariopsis*) were also most abundant at the northernmost stations, deepest into the ice pack during the ICESCAPE cruise (Laney and Sosik, 2014), presumably representative of an earlier UIB stage. The switch in dominance toward pelagic diatoms, in particular species of the centric diatom genera *Chaetoceros* and *Thalassiosira*, and in the case of N-ICE, *P. pouchetii*, coincided with the snow melt onset and a large lead fraction, respectively, and water column stratification. The notable exception is the Resolute Passage 2011 UIB which remained dominated by pennate diatoms (*Fossula arctica*, *Fragilariopsis cylindrus*, *F. oceanica*, and *Nitzschia frigida*) throughout (see "Box 2: Other Under-Ice Bloom Scenarios"). *Chaetoceros*, *Thalassiosira*, and *Phaeocystis* usually dominate the spring bloom along the Arctic continental margin (Degerlund and Eilertsen, 2010). In particular, spore-forming species of the former two diatom genera [e.g., *Chaetoceros gelidus* (formery *Chaetoceros socialis*), *Thalassiosira hyalina* and *Thalassiosira antarctica* var. *borealis*] are important bloom formers that exhibit a boom-and-bust life cycle and can increase biomass from background to bloom levels within 2–3 weeks. The comparably low *Chaetoceros* and *Thalassiosira* abundances in the deep central AO during the North Pole expedition 2015 suggest that, in addition to the low nutrient levels, these taxa might also be limited by dispersal of resting spores from the shallow

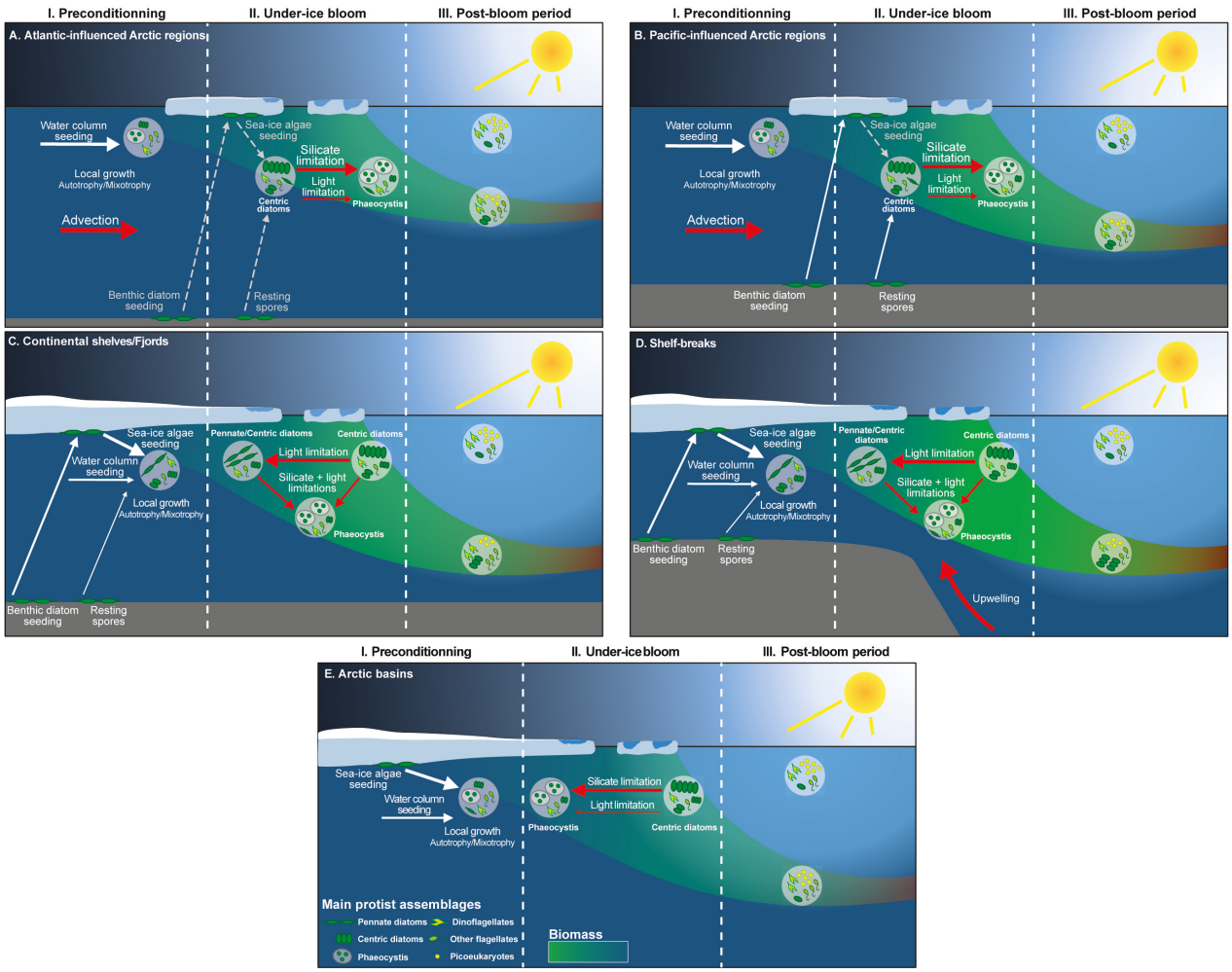

FIGURE 8 | Schematic drawing of different **(A–E)** under-ice phytoplankton blooms. The development of UIBs is divided in three distinct phases, i.e., the preconditioning, the under-ice bloom and the post-bloom period. The three potential seeding sources for UIBs are shown by the white arrows: algal cells in the water column, vegetative cells or resting stages at the sediment surface, and algal cells or resting stages from sea ice. The main environmental drivers controlling UIB dynamics are indicated in red. The size of the arrows is related to the importance of the processes. The main protist assemblages are depicted in the different white circles. The phytoplankton biomass is related to the transparency of the shape of the vertical dynamics of phytoplankton assemblages. The sea ice, water, and bottom compartments are also displayed.

shelves. Interestingly, an "UIB" dominated by *Chaetoceros* and *Thalassiosira* species was also observed during the Russian drift station North Pole 22 from May to October 1975 (Belyaeva, 1980) following formation of melt ponds on top of the MYI, similar to that observed in the late 1950s (**Figure 1**, Apollonio, 1959; English, 1961). However, maximum centric diatom abundances in 1975 were two orders of magnitude lower and about one month later (late August) than during the North Pole expedition 2015. The general trend toward stronger dominance of cryopelagic and pelagic diatom species in the more recent years is also supported by a study covering the MYI to FYI transition in the central AO over the last 40 years (Hop et al., 2020).

The general patterns described above are consistent with observations of UIBs in Baffin Bay in 2015 and 2016 during the Green Edge project (Oziel et al., 2019) with dominance of pennate diatoms and dinoflagellates during the early stages of UIBs and dominance of pelagic centric diatoms during the peak of the UIB. Notable exceptions are cryopelagic species belonging to the pennate diatom genera *Fragilariopsis* and *Pseudo-nitzschia*, which thrive both in sea ice and the water column (Hop et al., 2020), but are nevertheless usually outnumbered by centric diatoms of the genera *Chaetoceros* and *Thalassiosira* during the peak UIB phase.

Fate of UIBs

Intense grazing pressure is able to decimate phytoplankton biomass during the bloom peak or post-bloom phases (Sakshaug, 2004). Such large grazing pressure observed in summer requires a copepod community dominated by stage-V copepodites or adults which are relatively low in number during the early phase of an UIB (Sakshaug, 2004; Søreide et al., 2010; Daase et al., 2013). However, the UIB development is generally preceded by an ice algal bloom on which some zooplankton species are able

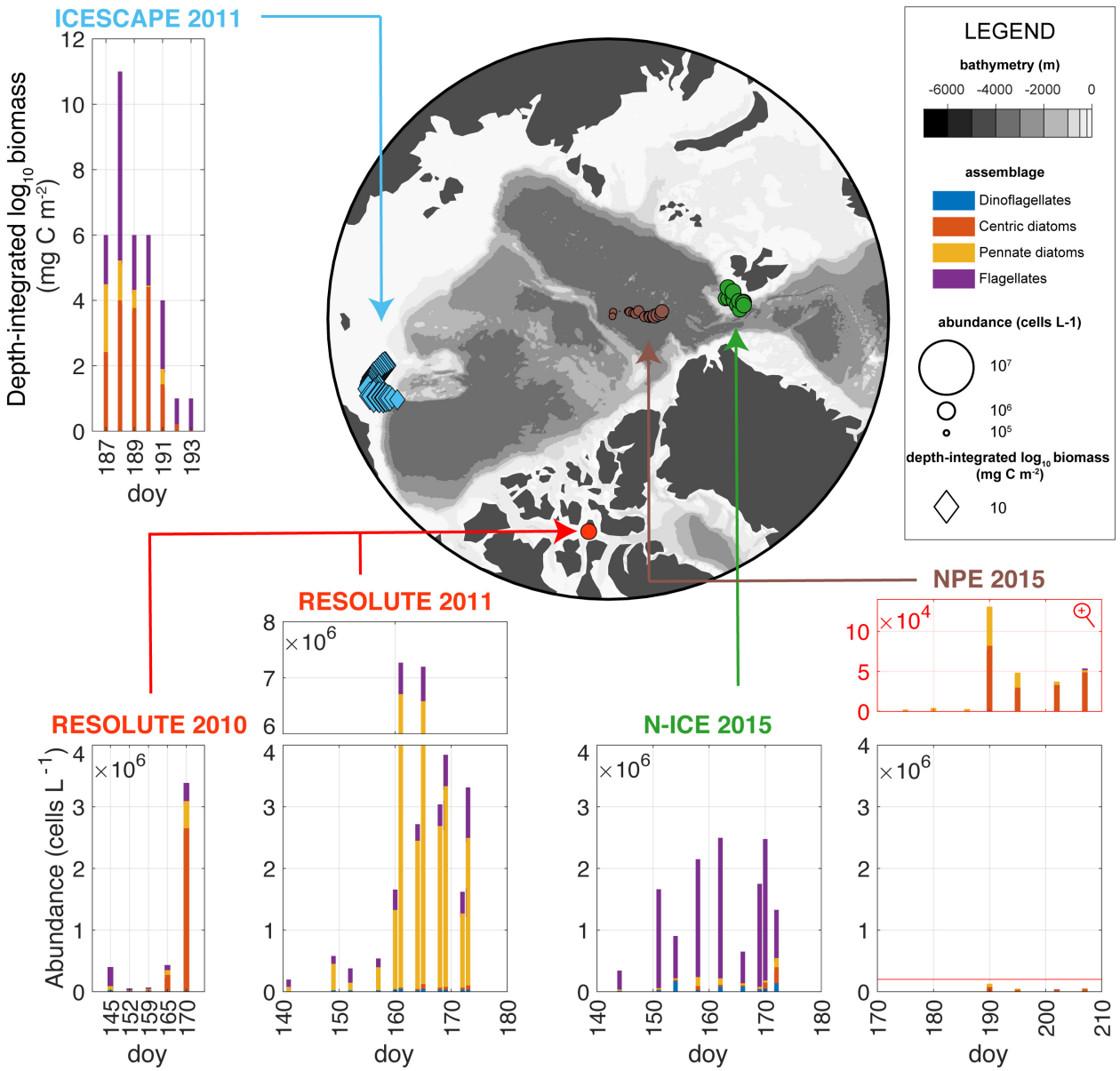

FIGURE 9 | Under-ice phytoplankton assemblages. The map displays the spatially distributed taxonomic inventories for each station and each expedition. The bar plots show the taxonomic inventories. Integrated biomass (diamonds in the map) was measured for ICESCAPE 2011 and abundances (circles in the map) for the rest of the expeditions. The main assemblages are shown, i.e., centric and pennate diatoms, dinoflagellates, and flagellates. Note that N-ICE flagellates were dominated by *Phaeocystis* which was not separately counted in the other studies. Phytoplankton abundances for N-ICE 2015, NPE 2015, Resolute 2010, and 2011 are representative of the upper 2–10 m of the under-ice water column while phytoplankton biomass for ICESCAPE 2011 was integrated over a maximum depth of 41 meters. doy, day of year.

to feed (Tourangeau and Runge, 1991; Wassmann and Slagstad, 1993; Hirche and Kosobokova, 2003; Wassmann et al., 2006; Søreide et al., 2008). Fortier et al. (2002) demonstrated that zooplankton can also feed well on released ice algae. Still, the time period of the developing UIB is often associated with a high flux of particulate organic carbon, mostly mediated by vertical sinking of ungrazed phytoplankton and ice algal cells (Fortier et al., 2002; Arrigo et al., 2014; Lalande et al., 2014, 2019). Similarly, Tamelander et al. (2008) suggested that ice algae can be an early food source for zooplankton and that the subsequent intense phytoplankton production exceeds the zooplankton grazing capacity, inducing a tight pelagic-benthic coupling. Overall, this suggests that in the early phase of an UIB, zooplankton are swamped by the abrupt increase in concentration and vertical flux of phytoplankton biomass. Hence, UIBs may represent an important and valuable food source for zooplankton grazers, including early recruitment stages, but they are likely not being controlled by grazing. In addition, sinking

of UIB biomass could be an important food source for benthic ecosystems, especially on the shallow continental shelves. Export of a *Phaeocystis*-dominated UIB to the seafloor of the continental shelf north of Svalbard was significantly enhanced by ballasting of *Phaeocystis* aggregates by gypsum minerals released from melting sea ice (Wollenburg et al., 2018). Recent observations of mass sedimentation of the mat-forming sea-ice diatom *Melosira arctica* to the deep-sea floor of the central AO during the record summer sea ice minimum year 2012 suggest that cryopelagic-benthic coupling might be enhanced under the new Arctic sea ice regime (Boetius et al., 2013).

PERSPECTIVES

Sea-ice loss is the most prominent manifestation of climate-driven changes in the AO. The combined effect of advanced summer sea-ice melt, MYI disappearance (in terms of extent, thickness and volume; Kwok, 2018), and increase in storm frequency and intensity (Graham et al., 2017; Rinke et al., 2017) will strengthen atmospheric forcing on surface Arctic waters. It will promote wind-induced shelf-break upwelling and mixing events (**Figure 6A**; Pickart et al., 2013) but will also accelerate the demise of sea ice itself (Graham et al., 2019). Thinning sea ice, reduced snow cover, increased presence of melt ponds (generally associated with FYI), and/or increased lead formation will also increase under-ice light availability which could support larger UIBs under FYI (**Figures 6C,D**; see also Horvat et al., 2017). Such an increase in bloom magnitude could, however, be mitigated by the still uncertain increase in snow precipitation over the Arctic (Bintanja, 2018; Webster et al., 2018) and by nutrient limitation in the central AO (Codispoti et al., 2013; Fernández-Méndez et al., 2015). In contrast, there is also potential for increased rain precipitation earlier in the season (Bintanja and Andry, 2017), that can trigger mass release of the spring ice algal community and lead to a relatively short-lived and fast-sinking pennate diatom UIBs (see "Box 2: Other Under-Ice Bloom Scenarios"). Common among all scenarios is the likely increased pelagic-benthic coupling as a result of an earlier bloom with minimal top-down influence.

Sea-ice loss has also direct influences on the hydrodynamical conditions of the AO (**Figure 7**). Recent studies have shown an overall intensification of AO circulation. According to altimetric-derived satellite observations, surface geostrophic currents have doubled in both the Arctic basin (2003–2014; Armitage et al., 2017) and in the European sub-Arctic area (1993–2016; Oziel et al., 2020). The increased Atlantic inflow is suspected to be mainly driven by reduced sea-ice export through the Greenland Sea, resulting in lower sea surface height and intensified cyclonic gyre activity in the Nordic Seas (Wang et al., 2020). The Atlantic inflow is also largely affected by upstream alteration in the North Atlantic such as the increased influence of the sub-tropical waters due to the weakening of the sub-polar gyre (Hátún et al., 2017), which is responsible for the reduced nutrient concentrations, especially silicates, in the Nordic Seas (Rey, 2012). The overall intensification of the surface circulation will increase the potential for advection of new nutrients and organisms (Vernet et al., 2019), especially along the topographically constrained boundary currents (see **Figure 6B**). In general, the AO will be more dynamic, and because it is also baroclinically unstable, more meso-scale features will be produced (e.g., eddies, meanders, fronts). Consistent with this, the expansion and shift of the Beaufort Gyre (Regan et al., 2019) due to increased freshwater accumulation (+40% since 1970, Proshutinsky et al., 2019) is accompanied by an increase in eddy activity (Zhao et al., 2014, 2016; Armitage et al., 2020) and interruptions of the transpolar drift due to accelerating sea-ice melt (Krumpen et al., 2019). Over 2001–2014, annual Bering Strait volume transport from the Pacific to the AO almost doubled as well (0.7×10^6 to 1.2×10^6 m^3 s^{-1}; Woodgate, 2018).

Therefore, the rapid transformation of local water masses due to the increased addition of freshwater and Atlantic- and Pacific-derived waters will alter the large-scale AO stratification. Arctic stratification will determine to a large extent nutrient availability in the surface euphotic layer (Tremblay and Gagnon, 2009, Ardyna et al., 2011) and constrain the magnitude of UIBs (Ardyna et al., 2020). Stratification is expected to increase in the Beaufort Gyre (Toole et al., 2010; **Figure 6A**) but decrease in other regions (e.g., in the European sector; Polyakov et al., 2017; Lind et al., 2018; **Figure 6B**) for different reasons (i.e., increased advection, mesoscale activity, atmospheric forcing, and related processes such as upwelling). The fate of freshwater will ultimately depend on the atmospheric and ocean circulation, which has been mainly in an anticyclonic regime during the last two decades, allowing freshwater accumulation (Haine et al., 2015). However, if the atmospheric circulation over the AO were to shift to a cyclonic regime, freshwater export may increase and ultimately alter the UIB dynamics.

BOX 1: NEW TECHNOLOGIES: MORE INSIGHTS ON UNDER-ICE BIOGEOCHEMICAL CYCLES AND BLOOMS

Our understanding of UIBs in a changing Arctic environment is based on few year-round and multiannual observations at specific locations. Additional long-term monitoring programs are clearly required, as well as large scale and/or high spatial resolution data to study spatial variability and distribution of Arctic UIBs. In view of these requirements, it is generally recognized that autonomous observing systems are well suited to provide observations at spatio-temporal resolutions previously hard to assess in the AO (Lee et al., 2017; Smith et al., 2019; **Figure 10**), especially during the winter-spring and summer-fall transitions when sea ice is present.

The Argo Program, which maintains a global array of autonomous and freely drifting profiling floats, is extending its array into Arctic regions (Jayne et al., 2017; Roemmich et al., 2019). All Argo floats carry conductivity-temperature-depth (CTD) sensors to measure accurate vertical temperature and salinity profiles mostly between 1000 and

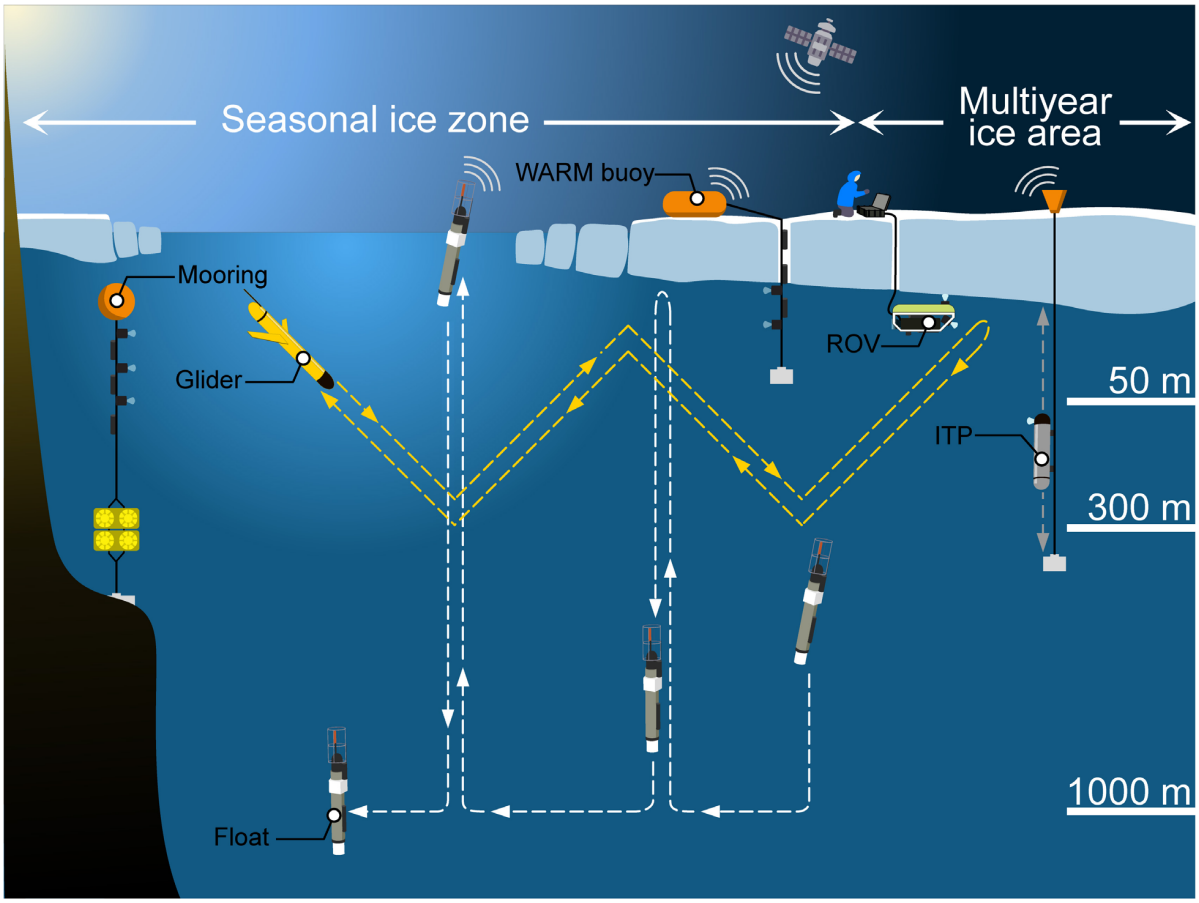

FIGURE 10 | Under-ice observing systems. Schematic drawing of different observing systems that can be used to study spatial variability and distribution of Arctic UIBs: floats, gliders, moorings, ITPs, ROVs, and WARM buoys. Modified from artwork in Sansoulet et al. (2019).

2000 m to the surface, every 5–10 days and for several years (Argo Steering Team, 1998). Several of them, called biogeochemical (BGC)-Argo floats, are equipped with additional sensors measuring other essential ocean variables (EOVs): Chl *a* concentration, suspended particles, oxygen concentration, nitrate concentration, pH, and/or downwelling irradiance (Biogeochemical-Argo Planning Group, 2016). These BGC-Argo core variables are quantified with operational and robust sensors, as well as with new and under development technologies (e.g., a miniaturized version of the Underwater Vision Profiler, Lombard et al., 2019; an underwater sea-ice detection sensor based on laser polarimetry, Lagunas et al., 2018). Recently, it has become possible to deploy BGC-Argo floats into seasonally ice-covered Arctic areas to study UIBs (Mayot et al., 2018; Randelhoff et al., 2020). While operating beneath the sea-ice cover, profiling floats collect vertical profiles of key biogeochemical variables, and transmit data after surfacing in open water. The presence of sea ice makes it difficult to geolocate ARGO float platforms, so under-ice trajectories are estimated using interpolation methods (Wallace et al., 2020). In order to prevent risk of colliding with sea ice, floats stop their ascent at 10 m and cannot provide near-surface information.

Other autonomous observing systems exist to study UIBs in seasonal ice zones, one of them being the Warming and Irradiance Measurements (WARM) buoy system (Hill et al., 2018; **Figure 10**). At deployment time in early spring, the float is placed on the surface of the ice and the cable lowered through a hole that is re-filled with ice and snow. After the sea ice melts in summer, the observing system is floating in open water until the next ice formation cycle begins in late fall. Similarly, UIBs can be studied with moorings deployed, for example, in fjords and equipped with analogous physical and bio-optical sensors (Leu et al., 2011). However, recorded data are mostly available only after the mooring is recovered.

In areas with multiyear ice, data transmission by Autonomous Underwater Vehicles (AUVs, e.g., gliders) is nearly impossible due to the lack of open water for surfacing. Ice-borne observing systems are preferentially deployed in such environments. For example, Ice-Tethered Profilers (ITPs) equipped with similar sensors as BGC-Argo floats can be used to study processes associated with UIBs (Krishfield et al., 2006; Berge et al., 2016; Laney et al., 2017; Boles et al., 2020). These platforms can provide multiannual datasets with a high-temporal resolution, as demonstrated by data collected in the Arctic Transpolar

Drift and the Beaufort Sea (Laney et al., 2014). Such long-term monitoring is possible thanks to engineering efforts to improve buoy survivability in thin ice, during ridging events and seasonal freeze-up.

Other autonomous observing systems can be deployed during ice camps or ship surveys, in order to provide high temporal and/or spatial resolution datasets of UIB-related processes. AUV platforms equipped with physical and bio-optical sensors were deployed in marginal ice zones in Baffin Bay (Green Edge project with glider platforms) and north of Svalbard (Johnsen et al., 2018). Surveys of the under-ice environment have been increasingly undertaken with remotely operated vehicles (ROVs). ROVs enable remote sensing of difficult to access locations across a range of temporal and spatial resolutions and minimize the disturbance of the ice environment in contrast to traditional ice coring techniques. Observational capabilities of ROVs are manifold due to a wide variety of attached sensors performing physical, chemical, and biological measurements (Katlein et al., 2017), and deployment distances from several hundred meters to extreme tether lengths of 20 km beneath the sea-ice cover (Nereid-UI ROV, Bowen et al., 2014; McFarland et al., 2015). For the investigation of parameters driving UIBs in Arctic waters, ROVs equipped with spectral radiometers have been frequently used to map under-ice irradiance and transmittance beneath landfast sea ice and moving pack ice in the AO (Nicolaus et al., 2012; Nicolaus and Katlein, 2013; Katlein et al., 2014, 2015, 2019; Lund-Hansen et al., 2018; Matthes et al., 2020).

As an example of the efficiency of autonomous platforms in providing broad spatial coverage, recently deployed autonomous instruments all around the Arctic show the anticipated latitudinal gradient in annual Chl *a* accumulation (**Figure 11**). Because annual maximum values of measured Chl *a* concentrations ranged from 0.2–0.5 mg m^{-3} for ITP platforms to 7–20 mg m^{-3} for floats and WARM buoys, these annual time series were normalized to their local annual maximum Chl *a* concentration value in order to focus on the phenology of UIBs. According to these time series, accumulation of phytoplankton biomass beneath mobile sea ice first occurred at the southernmost locations (e.g., in April for the Greenland Sea, Mayot et al., 2018; end of May for the Chukchi Sea, Hill et al., 2018) and 1–2 months later at northern Arctic locations (>85°N, Beaufort Sea, Laney et al., 2014; Amundsen-Nansen Basins, Boles et al., 2020).

Moreover, such annual cycle observations by autonomous systems revealed that significant phytoplankton biomass can accumulate in late spring after the melt onset, showing values as high as 15–40% of the annual maximum value observed in summer (**Figure 11**). These early increases in phytoplankton biomass frequently show short-term fluctuations. Upcoming concurrent measurements of Chl *a* concentration, water column mixing, PAR, and nitrate concentrations over a full annual cycle from more frequently deployed autonomous sampling platforms are needed to link and quantify the contribution of each individual bottom-up process to the observed short-term fluctuation in phytoplankton biomass. As pointed out by Laney et al. (2014), the impact of ice-algal Chl *a* on the Chl *a* fluorescence signal measured in the water column needs to be evaluated. Upward-looking cameras mounted on autonomous platforms can provide qualitative pictures of the ice–water interface and detect, for example, sinking aggregates of ice algae (e.g., Katlein et al., 2015; Hill et al., 2018; Johnsen et al., 2018). Finally, the drift of autonomous sampling platforms over large distances creates difficulties in the observation of UIBs in mobile pack ice over longer time periods. Some observed short-term fluctuations may be the result of the spatial variability in measurements from the drifting observing system used. An improved ocean observational effort in the pan-AO with an increased number of autonomous observing systems might overcome this issue (Smith et al., 2019).

BOX 2: OTHER UNDER-ICE BLOOM SCENARIOS

Here we briefly outline UIB scenarios that do not follow the "classical" UIB development as defined in the introduction.

UIBs During the Pre-melt Season

Although somewhat more moderate in terms of bloom magnitude, UIBs have been reported during the pre-melt season below sea ice with thin to moderate snow cover (<15 cm) in the Chukchi Sea (Lowry et al., 2018) or sea ice with thick snow cover (>40 cm) but an extensive fraction of open leads or leads covered by thin ice with thin snow cover in the Atlantic sector north of Svalbard (Assmy et al., 2017). However, in both cases, reduced vertical mixing and initiation of surface stratification, respectively, was a prerequisite for the UIB to form while extensive lead fraction under cold spring atmospheric forcing inhibited UIB formation due to convective mixing in refreezing leads (Lowry et al., 2018). Thus, water column stability, either induced by a stable water column below ∼100% sea-ice cover (no leads) (Lowry et al., 2018) or ceased convective mixing after leads have fully refrozen, in combination with Atlantic warm water influence on under-ice mixing processes (Assmy et al., 2017) are necessary conditions for UIBs to develop during the pre-melt season. In addition, the low but variable light conditions under the heavily snow-covered sea ice, crisscrossed with leads north of Svalbard, favored *P. pouchetii* over diatoms, facilitated by the high photosynthetic plasticity of the former species (Assmy et al., 2017).

UIBs Triggered by Extreme Meteorological Events

Depending on the mode of ice algal bloom termination, UIBs can be dominated by ice algae that continue growing in the water column and hence differ in bloom composition from the "classical" UIBs. A study from Resolute Passage in the Canadian Arctic Archipelago conducted in 2011 showed that rainfall triggered a rapid sloughing event of ice algae, dominated by pennate diatoms, followed by a pennate diatom-dominated bloom of the same species in the under-ice water column (Galindo et al., 2014). These observations were in contrast to the slower 3-week melt progression that led to an UIB dominated by centric diatoms of the genera *Thalassiosira* and *Chaetoceros* in the same region during the previous year

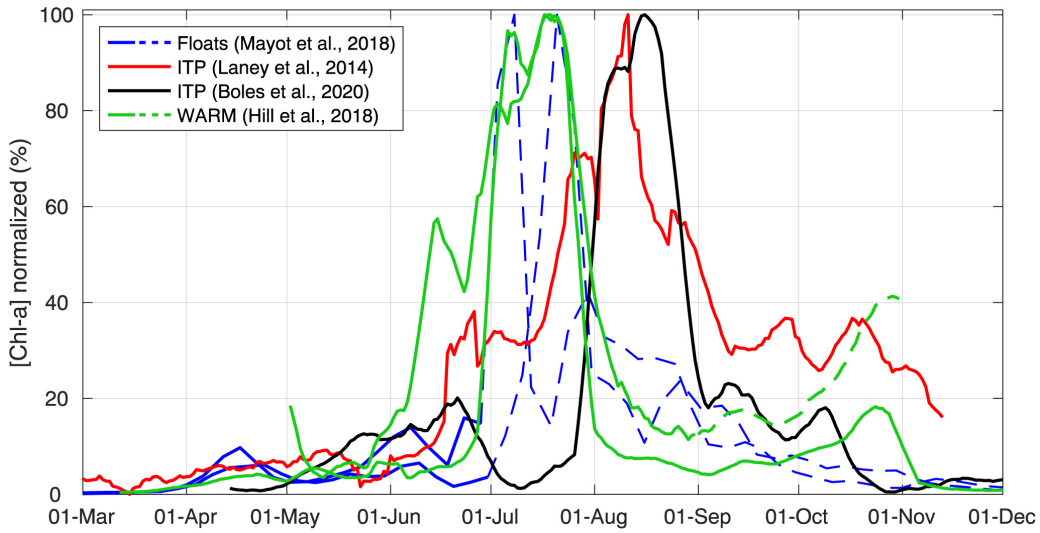

FIGURE 11 | Under-ice annual cycles of chlorophyll *a* concentration. Annual cycles of chlorophyll *a* concentration (proxy for phytoplankton biomass) collected under ice by different autonomous observing systems at different latitudes in the Arctic (~73°N in Greenland Sea: Mayot et al., 2018; >85°N in Beaufort Sea: Laney et al., 2014; ~85°N Amundsen-Nansen Basin: Boles et al., 2020; ~73°N in Chukchi Sea: Hill et al., 2018). All annual cycles have been normalized (divided by their annual maximum values) and smoothed with a 10-days moving average. Data from floats and ITP platforms correspond to the average values collected between 25–35 m. Data from WARM buoys were collected at 5 m. For floats and WARM buoy time series, dashed lines represent periods when platforms were not sampling under ice.

(Mundy et al., 2014). In 2014 during another rapid melt event in Cambridge Bay, the planktonic diatom composition at the beginning of an UIB was very close to that of the ice algal community (C.J. Mundy, unpublished data), which was dominated by the pennate diatom *N. frigida* and the centric diatom *Attheya* sp. (Campbell et al., 2017). Thus, it is possible that the onset of the bloom was seeded in part by ice algae sloughing from the ice bottom. These observations led to the hypothesis that rapid surface melt rates caused by, e.g., a rain event, can influence the dominant taxa of an UIB via sea-ice seed populations (Galindo et al., 2014). Similar observations of UIBs dominated by pennate sea-ice diatoms of the genera *Nitzschia*, *Fragilariopsis*, and *Navicula* were made in Resolute Passage in 1994 and 1995 after a rain event and a heat wave, respectively, which led to rapid release of ice algae into the under-ice water column (Fortier et al., 2002). These results suggest that seeding from sea ice plays a minor role for UIB development, unless mass release of ice algae into the water column is triggered by extreme meteorological events (Fortier et al., 2002; Galindo et al., 2014). This is consistent with findings by Selz et al. (2018), based on *in situ* observations collected in the Chukchi and Beaufort Seas, suggesting that the sloughing of ice algae into the water column can only briefly increase the phytoplankton biomass. Ice algae have a high aggregation potential due to their sticky nature and high concentrations of gelatinous extracellular polymeric substances in sea ice (Krembs et al., 2002; Riedel et al., 2006; Meiners et al., 2008) leading to much lower residence time in the water column as compared to suspended phytoplankton (Riebesell et al., 1991). Such release events could partly explain observed short-term fluctuations in Chl *a* concentrations measured under ice in spring by autonomous platforms (see "Box 1: New technologies: More insights on under-ice biogeochemical cycles and blooms").

Sea-Ice Meltwater UIBs

Other UIBs are restricted to the oligotrophic meltwater layer just below the sea ice (under-ice melt ponds *sensu* Gradinger, 1996) and usually numerically dominated by phytoflagellates belonging to the prasinophytes, prymnesiophytes, and/or chrysophytes (Gradinger, 1996; Mundy et al., 2011). Similar UIBs restricted to the upper 2 m below the sea ice and dominated by phytoflagellates, termed halocline flora, were observed by Bursa (1963) and Apollonio (1985) but characterized by a different species composition (*Chlorella* sp., *Oocystis* sp., *Scenedesmus bijugatus*, and *Ochromonas* sp.) and generally lower biomass. Although hosting an active microbial community, these under-ice melt pond assemblages are often dominated by few or even a single species and are distinctly different from the pennate diatom community dominating the bottom of sea ice (Gradinger, 1996). However, seeding from sea ice seems to play an important role in the initial stages of these UIBs until a unique community characteristic to this environment develops (Mundy et al., 2011). The vertical extent of these blooms is restricted to a few meters compared to the UIBs described above, which usually occupy tens of meters in the upper surface mixed layer. Even thinner (<1 mm) yet dense accumulations of up to 117 mg Chl *a* m^{-3} of the phototrophic ciliate *Mesodinium rubrum* at the ice–water interface, reminiscent of red tides of this species in open waters of temperate to tropical seas, have been observed below newly formed sea ice with little snow cover (Olsen et al., 2019). The highly motile and phototactic behavior of this ciliate in combination with convective mixing caused by brine rejection

in growing sea ice enabled *M. rubrum* to bloom at the ice–water interface as long as the sea ice was growing.

AUTHOR CONTRIBUTIONS

MA and CM led the design of the study. CM, NM, LM, LO, and CH made the figures. LO and CH conducted the analysis. All authors revised the earlier version of the manuscript, helped in the interpretation, and approved the final version for publication.

FUNDING

MA was supported by a European Union's Horizon 2020 Marie Skłodowska-Curie grant (no. 746748). CM's contribution was supported by a Natural Sciences and Engineering Council of Canada (NSERC) Discovery grant and an NSERC grant as part of the Belmont Forum/BiodivERsA project entitled De-icing of Arctic Coasts: Critical or new opportunities for marine biodiversity and Ecosystem Services? (ACCES). PM and NM were funded by NASA award 80NSSC18K0081 P00004. LM was supported by a University of Manitoba Graduate Student Fellowship. CH thanks the Institute of Water and Atmospheric Science in New Zealand for their hospitality and acknowledges support from the Voss Postdoctoral Fellowship at Brown University and NASA Grant GR5227091. LO's contribution was funded by the Nunataryuk project from the European Union's Horizon 2020 Research and Innovation Programme under grant agreement no. 773421. EL's contribution was funded through the project FAABulous: Future Arctic Algae Blooms—and their role in the context of climate change (Research Council of Norway, project grant nr. 243702). PA's contribution was funded by the former Centre for Ice, Climate and Ecosystems at the Norwegian Polar Institute, the project "Boom or Bust: Ice-algal and under-ice phytoplankton bloom dynamics in a changing Arctic icescape" (Research Council of Norway grant nr. 244646), and the Arktis 2030 program of the Ministries of Foreign Affairs and Climate and Environment of Norway, through the project ID Arctic. VH's contribution was funded through NSF Office of Polar Programs grants 1203784 and 1603548. IM's contribution was supported by Russian Federation project #0149-2018-0009 and Russian Federation for Basic Research project #18-05-00099. KA's contribution was supported by the NSF Office of Polar Programs grant PLR-1304563.

ACKNOWLEDGMENTS

This synthesis work represents a contribution of the fourth pan-Arctic symposium (organized by Paul Wassmann in Motovun, Croatia). We would like to express our gratitude to the participants of this symposium for their discussions and feedback during early formative stages of this work.

REFERENCES

Apollonio, S. (1959). Hydrobiological measurements on IGY Drifting Station Bravo. *Natl. Acad. Sci. IGY Bull.* 27, 16–19.

Apollonio, S. (1985). Arctic marine phototrophic systems: functions of sea ice stabilisation. *Arctic* 38, 167–173.

Apollonio, S., and Matrai, P. (2011). Marine primary production in the Canadian Arctic, 1956, 1961–1963. *Polar Biol.* 34, 767–774. doi: 10.1007/s00300-010-0928-3

Ardyna, M., Babin, M., Devred, E., Forest, A., Gosselin, M., Raimbault, P., et al. (2017). Shelf-basin gradients shape ecological phytoplankton niches and community composition in the coastal Arctic Ocean (Beaufort Sea). *Limnol. Oceanogr.* 62, 2113–2132. doi: 10.1002/lno.10554

Ardyna, M., Gosselin, M., Michel, C., Poulin, M., and Tremblay, J.-É. (2011). Environmental forcing of phytoplankton community structure and function in the Canadian High Arctic: contrasting oligotrophic and eutrophic regions. *Mar. Ecol. Prog. Ser.* 442, 37–57. doi: 10.1002/lno.10554

Ardyna, M., Mundy, C., Mills, M. M., Lacour, L., Oziel, L., Grondin, P. L., et al. (2020). Environmental drivers of under-ice phytoplankton bloom dynamics in the Arctic Ocean. *Elem. Sci. Anth.* 8:30. doi: 10.1525/elementa.430

Argo Steering Team (1998). *On The Design and Implementation of Argo: A Global Array of Profiling Floats*. San Diego, CA: Argo Steering Team.

Armitage, T. W. K., Bacon, S., Ridout, A. L., Petty, A. A., Wolbach, S., and Tsamados, M. (2017). Arctic Ocean surface geostrophic circulation 2003–2014. *Cryosphere* 11, 1767–1780. doi: 10.5194/tc-11-1767-2017

Armitage, T. W. K., Manucharyan, G. E., Petty, A. A., Kwok, R., and Thompson, A. F. (2020). Enhanced eddy activity in the Beaufort Gyre in response to sea ice loss. *Nat. Commun.* 11:761.

Arrigo, K. R., Mills, M. M., Dijken, G. L., Lowry, K. E., Pickart, R. S., and Schlitzer, R. (2017). Late spring nitrate distributions beneath the ice-covered Northeastern Chukchi Shelf. *J. Geophys. Res. Biogeosci.* 122, 2409–2417. doi: 10.1002/2017jg003881

Arrigo, K. R., Mills, M. M., Kropuenske, L. R., van Dijken, G. L., Alderkamp, A.-C., and Robinson, D. H. (2010). Photophysiology in two major Southern Ocean Phytoplankton Taxa: photosynthesis and growth of *Phaeocystis antarctica* and *Fragilariopsis cylindrus* under different irradiance levels. *Integr. Comp. Biol.* 50, 950–966. doi: 10.1093/icb/icq021

Arrigo, K. R., Perovich, D. K., Pickart, R. S., Brown, Z. W., van Dijken, G. L., Lowry, K. E., et al. (2012). Massive phytoplankton blooms under arctic sea ice. *Science* 336, 1408–1408.

Arrigo, K. R., Perovich, D. K., Pickart, R. S., Brown, Z. W., van Dijken, G. L., Lowry, K. E., et al. (2014). Phytoplankton blooms beneath the sea ice in the Chukchi Sea. *Deep Sea Res.* 105, 1–16.

Arrigo, K. R., Sullivan, C. W., and Kremer, J. N. (1991). A bio-optical model of Antarctic sea ice. *J. Geophys. Res. Oceans* 96, 10581–10592. doi: 10.1029/91jc00455

Assmy, P., Fernández-Méndez, M., Duarte, P., Meyer, A., Randelhoff, A., Mundy, C. J., et al. (2017). Leads in Arctic pack ice enable early phytoplankton blooms below snow-covered sea ice. *Sci. Rep.* 7:40850.

Back, D. Y., Ha, S., Else, B., Hanson, M., Jones, S. F., Shin, K., et al. (2020). On the impact of wastewater effluent on phytoplankton in the Arctic coastal zone: a case study in the Kitikmeot Sea of the Canadian Arctic. *Sci. Total Environ.* (in press).

Bélanger, S., Babin, M., and Tremblay, J. -É (2013). Increasing cloudiness in Arctic damps the increase in phytoplankton primary production due to sea ice receding. *Biogeosciences* 10, 4087–4101. doi: 10.5194/bg-10-4087-2013

Belyaeva, T. V. (1980). "Phytoplankton in the drift area of the station North Pole-22", in *Biology of the Central Arctic Basin*, eds. M. E. Vinogradov and I. A. Melnikov (Moscow: Nauka), 133–143.

Berge, J., Geoffroy, M., Johnsen, G., Cottier, F., Bluhm, B., and Vogedes, D. (2016). Ice-tethered observational platforms in the Arctic Ocean pack ice. *IFAC Pap OnLine* 49, 494–499. doi: 10.1016/j.ifacol.2016.10.484

Bintanja, R. (2018). The impact of Arctic warming on increased rainfall. *Sci. Rep.* 8:16001.

Bintanja, R., and Andry, O. (2017). Towards a rain-dominated Arctic. *Nat. Clim. Change* 7, 263–267. doi: 10.1038/nclimate3240

Biogeochemical-Argo Planning Group (2016). *The scientific rationale, design and Implementation Plan for a Biogeochemical-Argo float array*. France: IFREMER. doi: 10.13155/46601

Błachowiak-Samołyk, K., Wiktor, J. M., Hegseth, E. N., Wold, A., Falk-Petersen, S., and Kubiszyn, A. M. (2015). Winter Tales: the dark side of planktonic life. *Polar Biol.* 38, 23–36. doi: 10.1007/s00300-014-1597-4

Boetius, A., Albrecht, S., Bakker, K., Bienhold, C., Felden, J., Fernández-Méndez, M., et al. (2013). Export of algal biomass from the melting Arctic sea ice. *Science* 339, 1430–1432. doi: 10.1126/science.1231346

Boles, E., Provost, C., Garçon, V., Bertosio, C., Athanase, M., Koenig, Z., et al. (2020). Under-ice phytoplankton blooms in the central Arctic Ocean: insights from the first biogeochemical IAOOS platform drift in 2017. *J. Geophys. Res. Oceans* 125:e2019JC015608.

Bowen, A. D., Yoerger, D. R., German, C. C., Kinsey, J. C., Jakuba, M. V., Gomez-Ibanez, D., et al. (2014). "Design of Nereid-UI: a remotely operated underwater vehicle for oceanographic access under ice", in *Proceeding of the 2014 Oceans*, St. John's, 1–6.

Braarud, T. (1935). *The "Øst" Expedition to the Denmark Strait, 1929*, Vol. 2. Oslo: Hvalrådets Skrifter. Nr.

Briegleb, B. P., and Light, B. (2007). "A Delta-Eddington multiple scattering parameterization for solar radiation", in *The Sea Ice Component of the Community Climate System Model Tech. Rep.* (Tirupati: National Center for Atmospheric Research).

Brown, T. A., Hegseth, E. N., and Belt, S. T. (2015). A biomarker-based investigation of the mid-winter ecosystem in Rijpfjorden, Svalbard. *Polar Biol.* 38, 37–50. doi: 10.1007/s00300-013-1352-2

Bursa, A. (1963). Phytoplankton in coastal waters of the Arctic Ocean at Point Barrow, Alaska. *Arctic* 16, 239–262. doi: 10.14430/arctic3544

Campbell, K., Mundy, C. J., Gosselin, M., Landy, J. C., Delaforge, A., and Rysgaard, S. (2017). Net community production in the bottom of first-year sea ice over the Arctic spring bloom. *Geophys. Res. Lett.* 44, 8971–8978. doi: 10.1002/2017gl074602

Carmack, E. C. (2007). The alpha/beta ocean distinction: a perspective on freshwater fluxes, convection, nutrients and productivity in high-latitude seas. *Deep Sea Res. Part II* 54, 2578–2598. doi: 10.1016/j.dsr2.2007.08.018

Carmack, E. C., and Chapman, D. C. (2003). Wind-driven shelf/basin exchange on an Arctic shelf: the joint roles of ice cover extent and shelf-break bathymetry. *Geophys. Res. Lett.* 30:1778.

Carmack, E. C., Macdonald, R. W., and Jasper, S. (2004). Phytoplankton productivity on the Canadian Shelf of the Beaufort Sea. *Mar. Ecol. Prog. Ser.* 277, 37–50. doi: 10.3354/meps277037

Castellani, G., Schaafsma, F. L., Arndt, S., Lange, B. A., Peeken, I., Ehrlich, J., et al. (2020). Large-scale variability of physical and biological sea-ice properties in polar oceans. *Front. Mar. Sci.* 7:536. doi: 10.3389/fmars.2020.00536

Codispoti, L. A., Kelly, V., Thessen, A., Matrai, P., Suttles, S., Hill, V., et al. (2013). Synthesis of primary production in the Arctic Ocean: III. Nitrate and phosphate based estimates of net community production. *Prog. Oceanogr.* 110, 126–150. doi: 10.1016/j.pocean.2012.11.006

Daase, M., Falk-Petersen, S., Varpe, Ø, Darnis, G., Søreide, J. E., Wold, A., et al. (2013). Timing of reproductive events in the marine copepod Calanus glacialis: a pan-Arctic perspective. *Can. J. Fish. Aquat. Sci.* 70, 871–884. doi: 10.1139/cjfas-2012-0401

Degerlund, M., and Eilertsen, H. C. (2010). Main species characteristics of phytoplankton spring blooms in NE Atlantic and Arctic Waters (68–80° N). *Estuar. Coast.* 33, 242–269. doi: 10.1007/s12237-009-9167-7

Devine, L., Kennedy, M. K., St-Pierre, I., Lafleur, C., Ouellet, M., and Bond, S. (2014). BioChem: the Fisheries and Oceans Canada database for biological and chemical data. *Can. Tech. Rep. Fish. Aquat. Sci.* 3073:40. doi: 10.1029/2018jc014045

Ehn, J. K., and Mundy, C. J. (2013). Assessment of light absorption within highly scattering bottom sea ice from under-ice light measurements: implications for Arctic ice algae primary production. *Limnol. Oceanogr.* 58, 893–902. doi: 10.4319/lo.2013.58.3.0893

Ehn, J. K., Mundy, C. J., Barber, D. G., Hop, H., Rossnagel, A., and Stewart, J. (2011). Impact of horizontal spreading on light propagation in melt pond covered seasonal sea ice in the Canadian Arctic. *J. Geophys. Res. Oceans* 116:C00G02.

Ehn, J. K., Papakyriakou, T. N., and Barber, D. G. (2008). Inference of optical properties from radiation profiles within melting landfast sea ice. *J. Geophys. Res. Oceans* 113:C09024.

Elliott, A., Mundy, C. J., Gosselin, M., Poulin, M., Campbell, K., and Wang, F. (2015). Spring production of mycosporine-like amino acids and other UV absorbing compounds in sea ice associated algae communities in the Canadian Arctic. *Mar. Ecol. Prog. Ser.* 541, 91–104. doi: 10.3354/meps11540

English, T. S. (1961). *Some Biological Observations in the Central North Polar Sea Drift Station Alpha, 1957-1958. Scientific Reports No. 15*. Calgary, AB: Arctic Institute of North America, 1–80.

Falk-Petersen, S., Pavlov, V., Berge, J., Cottier, F., Kovacs, K. M., and Lydersen, C. (2015). At the rainbow's end: high productivity fueled by winter upwelling along an Arctic shelf. *Polar Biol.* 38, 5–11. doi: 10.1007/s00300-014-1482-1

Fernández-Méndez, M., Katlein, C., Rabe, B., Nicolaus, M., Peeken, I., Bakker, K., et al. (2015). Photosynthetic production in the central Arctic Ocean during the record sea-ice minimum in 2012. *Biogeosciences* 12, 3525–3549. doi: 10.5194/bg-12-3525-2015

Fetterer, F., and Untersteiner, N. (1998). Observations of melt ponds on Arctic sea ice. *J. Geophys. Res. Oceans* 103, 24821–24835. doi: 10.1029/98jc02034

Fortier, M., Fortier, L., Michel, C., and Legendre, L. (2002). Climatic and biological forcing of the vertical flux of biogenic particles under seasonal Arctic sea ice. *Mar. Ecol. Prog. Ser.* 225, 1–16. doi: 10.3354/meps225001

Frey, K. E., Perovich, D. K., and Light, B. (2011). The spatial distribution of solar radiation under a melting Arctic sea ice cover. *Geophys. Res. Lett.* 38: L22501.

Galindo, V., Levasseur, M., Mundy, C. J., Gosselin, M., Tremblay, J. E., Scarratt, M., et al. (2014). Biological and physical processes influencing sea ice, under-ice algae, and dimethylsulfoniopropionate during spring in the Canadian Arctic Archipelago. *J. Geophys. Res. Oceans* 119, 3746–3766. doi: 10.1002/2013jc009497

Geider, R. J., MacIntyre, H. L., and Kana, T. M. (1998). A dynamic regulatory model of phytoplanktonic acclimation to light, nutrients, and temperature. *Limnol. Oceanogr.* 43, 679–694. doi: 10.4319/lo.1998.43.4.0679

Gosselin, M., Levasseur, M., Wheeler, P. A., Horner, R. A., and Booth, B. C. (1997). New measurements of phytoplankton and ice algal production in the Arctic Ocean. *Deep Sea Res. Part II* 44, 1623–1644. doi: 10.1016/s0967-0645(97)00054-4

Gradinger, R. (1996). Occurrence of an algal bloom under Arctic pack ice. *Mar. Ecol. Prog. Ser.* 131, 301–305. doi: 10.3354/meps131301

Graham, R. M., Cohen, L., Petty, A. A., Boisvert, L. N., Rinke, A., Hudson, S. R., et al. (2017). Increasing frequency and duration of Arctic winter warming events. *Geophys. Res. Lett.* 2017:GL073395.

Graham, R. M., Itkin, P., Meyer, A., Sundfjord, A., Spreen, G., Smedsrud, L. H., et al. (2019). Winter storms accelerate the demise of sea ice in the Atlantic sector of the Arctic Ocean. *Sci. Rep.* 9:9222.

Gran, E. H. (1904). Diatomaceae from the ice-floes and plankton of the Arctic Ocean. The Norwegian north polar expedition, 1893-1896. *Sci. Res.* 4, 1–74.

Ha, H. K., Kim, Y. H., Lee, H. J., Hwang, B., and Joo, H. M. (2015). Under-ice measurements of suspended particulate matters using ADCP and LISST-Holo. *Ocean Sci.* 50, 97–108. doi: 10.1007/s12601-015-0008-2

Haas, C., Beckers, J., King, J., Silis, A., Stroeve, J., Wilkinson, J., et al. (2017). Ice and snow thickness variability and change in the high Arctic Ocean observed by in-situ measurements. *Geophys. Res. Lett.* 44, 462–410.

Haine, T. W. N., Curry, B., Gerdes, R., Hansen, E., Karcher, M., Lee, C., et al. (2015). Arctic freshwater export: status, mechanisms, and prospects. *Glob. Planet. Change* 125, 13–35. doi: 10.1016/j.gloplacha.2014.11.013

Hátún, H., Azetsu-Scott, K., Somavilla, R., Rey, F., Johnson, C., Mathis, M., et al. (2017). The subpolar gyre regulates silicate concentrations in the North Atlantic. *Sci. Rep.* 7:14576.

Hegseth, E. N., Assmy, P., Wiktor, J. M., Wiktor, J., Kristiansen, S., Leu, E., et al. (2019). "Phytoplankton seasonal dynamics in kongsfjorden, svalbard and the adjacent shelf," in *The Ecosystem of Kongsfjorden, Svalbard*, eds H. Hop and

C. Wiencke (Cham: Springer International Publishing), 173–227. doi: 10.1007/978-3-319-46425-1_6

Hill, V. J., Cota, G., and Stockwell, D. (2005). Spring and summer phytoplankton communities in the Chukchi and Eastern Beaufort Seas. *Deep Sea Res. Part II* 52, 3369–3385. doi: 10.1016/j.dsr2.2005.10.010

Hill, V. J., Light, B., Steele, M., and Zimmerman, R. C. (2018). Light availability and phytoplankton growth beneath Arctic sea ice: integrating observations and modeling. *J. Geophys. Res. Oceans* 123, 3651–3667. doi: 10.1029/2017jc013617

Hirche, H. J., and Kosobokova, K. (2003). Early reproduction and development of dominant calanoid copepods in the sea ice zone of the Barents Sea—need for a change of paradigms? *Mar. Biol.* 143, 769–781. doi: 10.1007/s00227-003-1122-8

Hop, H., Vihtakari, M., Bluhm, B. A., Assmy, P., Poulin, M., Gradinger, R., et al. (2020). Changes in sea-ice protist diversity with declining sea ice in the Arctic Ocean from the 1980s to 2010s. *Front. Mar. Sci.* 7:243. doi: 10.3389/fmars.2020.00243

Horvat, C., Flocco, D., Rees jones, D. W., Roach, L., and Golden, K. M. (2020). The effect of melt pond geometry on the distribution of solar energy under first-year sea ice. *Geophys. Res. Lett.* 47:e2019GL085956.

Horvat, C., Jones, D. R., Iams, S., Schroeder, D., Flocco, D., and Feltham, D. (2017). The frequency and extent of sub-ice phytoplankton blooms in the Arctic Ocean. *Sci. Adv.* 3:e1601191. doi: 10.1126/sciadv.1601191

Huang, W., Lu, P., Lei, R., Xie, H., and Li, Z. (2016). Melt pond distribution and geometry in high Arctic sea ice derived from aerial investigations. *Ann. Glaciol.* 57, 105–118. doi: 10.1017/aog.2016.30

Hussherr, R., Levasseur, M., Lizotte, M., Tremblay, J. É, Mo, J., Thomas, H., et al. (2017). Impact of ocean acidification on Arctic phytoplankton blooms and dimethyl sulfide concentration under simulated ice-free and under-ice conditions. *Biogeosciences* 14, 2407–2427. doi: 10.5194/bg-14-2407-2017

Jackson, J. M., Melling, H., Lukovich, J. V., Fissel, D., and Barber, D. G. (2015). Formation of winter water on the Canadian Beaufort shelf: new insight from observations during 2009–2011. *J. Geophys. Res. Oceans* 120, 4090–4107. doi: 10.1002/2015jc010812

Jayne, S. R., Roemmich, D., Zilberman, N., Riser, S. C., Johnson, K. S., Johnson, G. C., et al. (2017). The argo program: present and future. *Oceanography* 30, 18–28. doi: 10.5670/oceanog.2017.213

Jimenez, V., Burns, J. A., Le Gall, F., Not, F., and Vaulot, D. (2020). No evidence of phago-mixotropy in *Micromonas polaris*, the dominant picophytoplankton species in the Arctic. *bioRxiv* doi: 10.1101/2020.05.26.117895

Johnsen, G., Leu, E., and Gradinger, R. (2020). "Marine micro- and macroalgae in the polar night," in *POLAR NIGHT Marine Ecology: Life and Light in the Dead of Night*, eds J. Berge, G. Johnsen, and J. H. Cohen (Cham: Springer International Publishing), 67–112. doi: 10.1007/978-3-030-33208-2_4

Johnsen, G., Norli, M., Moline, M., Robbins, I., Von Quillfeldt, C., Sørensen, K., et al. (2018). The advective origin of an under-ice spring bloom in the Arctic Ocean using multiple observational platforms. *Polar Biol.* 41, 1197–1216. doi: 10.1007/s00300-018-2278-5

Joy-Warren, H. L., Dijken, V. G. L., Alderkamp, A.-C., Leventer, A., Lewis, K. M., Selz, V., et al. (2019). Light is the primary driver of early season phytoplankton production along the Western Antarctic Peninsula. *J. Geophys. Res. Oceans* 124, 7375–7399. doi: 10.1029/2019jc015295

Katlein, C., Arndt, S., Belter, H. J., Castellani, G., and Nicolaus, M. (2019). Seasonal evolution of light transmission distributions through Arctic sea ice. *J. Geophys. Res. Oceans* 124, 5418–5435. doi: 10.1029/2018jc014833

Katlein, C., Fernández-Méndez, M., Wenzhöfer, F., and Nicolaus, M. (2015). Distribution of algal aggregates under summer sea ice in the Central Arctic. *Polar Biol.* 38, 719–731. doi: 10.1007/s00300-014-1634-3

Katlein, C., Nicolaus, M., and Petrich, C. (2014). The anisotropic scattering coefficient of sea ice. *J. Geophys. Res. Oceans* 119, 842–855. doi: 10.1002/2013jc009502

Katlein, C., Perovich, D. K., and Nicolaus, M. (2016). Geometric effects of an inhomogeneous sea ice cover on the under ice light field. *Front. Earth Sci.* 4:6. doi: 10.3389/feart.2016.00006

Katlein, C., Schiller, M., Belter, H. J., Coppolaro, V., Wenslandt, D., and Nicolaus, M. (2017). A new remotely operated sensor platform for interdisciplinary observations under sea ice. *Front. Mar. Sci.* 4:281. doi: 10.3389/fmars.2017.00281

Kauko, H. M., Pavlov, A. K., Johnsen, G., Granskog, M. A., Peeken, I., and Assmy, P. (2019). Photoacclimation state of an Arctic under-ice phytoplankton bloom. *J. Geophys. Res. Oceans* 124, 1750–1762. doi: 10.1029/2018jc014777

Kinney, C. J., Maslowski, W., Osinski, R., Jin, M., Frants, M., Jeffery, N., et al. (2020). Hidden production: on the importance of pelagic phytoplankton blooms beneath Arctic sea ice. *J. Geophys. Res. Oceans* 125:e2020JC016211.

Kirillov, S., Dmitrenko, I., Tremblay, B., Gratton, Y., Barber, D., and Rysgaard, S. (2016). Upwelling of Atlantic water along the Canadian Beaufort sea continental slope: favorable atmospheric conditions and seasonal and interannual variations. *J. Clim.* 29, 4509–4523. doi: 10.1175/jcli-d-15-0804.1

Krembs, C., Eicken, H., Junge, K., and Deming, J. W. (2002). High concentrations of exopolymeric substances in Arctic winter sea ice: implications for the polar ocean carbon cycle and cryoprotection of diatoms. *Deep Sea Res. Part II* 49, 2163–2181. doi: 10.1016/s0967-0637(02)00122-x

Krishfield, R., Doherty, K., Frye, D., Hammar, T., Kemp, J., Peters, D., et al. (2006). *Design and Operation of Automated Ice-Tethered Profilers for Real-Time Seawater Observations in the Polar Oceans*. WHOI Technical Reports 2006-06. Available online at: https://hdl.handle.net/1912/1170

Krumpen, T., Belter, H. J., Boetius, A., Damm, E., Haas, C., Hendricks, S., et al. (2019). Arctic warming interrupts the transpolar drift and affects long-range transport of sea ice and ice-rafted matter. *Sci. Rep.* 9:5459.

Kvernvik, A. C., Rokitta, S., Rost, B., Gabrielsen, T., Leu, E., and Hoppe, C. J. M. (2020). Higher sensitivity towards light stress and ocean acidification in an Arctic sea-ice associated diatom compared to a pelagic diatom. *New Phytol.* 226, 1708–1724. doi: 10.1111/nph.16501

Kvernvik, A. C., Hoppe, C. J. M., Lawrenz, E., Prasil, O., Greenacre, M., Wiktor, J. M., et al. (2018). Fast reactivation of photosynthesis in Arctic phytoplankton during the polar night. *J. Phycol.* 54, 461–470. doi: 10.1111/jpy.12750

Kwok, R. (2018). Arctic sea ice thickness, volume, and multiyear ice coverage: losses and coupled variability (1958–2018). *Environ. Res. Lett.* 13:105005. doi: 10.1088/1748-9326/aae3ec

Lacour, T., Morin, P.-I., Sciandra, T., Donaher, N., Campbell, D. A., Ferland, J., et al. (2019). Decoupling light harvesting, electron transport and carbon fixation during prolonged darkness supports rapid recovery upon re-illumination in the Arctic diatom *Chaetoceros neogracilis*. *Polar Biol.* 42, 1787–1799. doi: 10.1007/s00300-019-02507-2

Lagunas, J., Marec, C., Leymarie, É, Penkerc'h, C., Rehm, E., Desaulniers, P., et al. (2018). *Sea-ice Detection for Autonomous Underwater Vehicles and Oceanographic Lagrangian Platforms by Continuous-Wave Laser Polarimetry*. Bellingham, WA: SPIE.

Lalande, C., Nöthig, E. M., and Fortier, L. (2019). Algal export in the Arctic Ocean in times of global warming. *Geophys. Res. Lett.* 46, 5959–5967. doi: 10.1029/2019gl083167

Lalande, C., Nöthig, E.-M., Somavilla, R., Bauerfeind, E., Shevshenko, V., and Okolodkov, Y. (2014). Variability in under-ice export fluxes of biogenic matter in the Arctic Ocean. *Global Biogeochem. Cycle* 2013:GB004735.

Laney, S. R., Krishfield, R. A., and Toole, J. M. (2017). The euphotic zone under Arctic Ocean sea ice: vertical extents and seasonal trends. *Limnol. Oceanogr.* 62, 1910–1934. doi: 10.1002/lno.10543

Laney, S. R., Krishfield, R. A., Toole, J. M., Hammar, T. R., Ashjian, C. J., and Timmermans, M. L. (2014). Assessing algal biomass and bio-optical distributions in perennially ice-covered polar ocean ecosystems. *Polar Sci.* 8, 73–85. doi: 10.1016/j.polar.2013.12.003

Laney, S. R., and Sosik, H. M. (2014). Phytoplankton assemblage structure in and around a massive under-ice bloom in the Chukchi Sea. *Deep Sea Res. Part II* 105, 30–41. doi: 10.1016/j.dsr2.2014.03.012

Lee, C. M., Thomson, J., Cho, K. H., Cole, S., Doble, M., Freitag, L., et al. (2017). An autonomous approach to observing the seasonal ice zone in the western Arctic. *Oceanography* 30, 56–68. doi: 10.5670/oceanog.2017.222

Legendre, L., Ingram, R. G., and Poulin, M. (1981). Physical control of phytoplankton production under sea ice (Manitounuk Sound, Hudson Bay). *Can. J. Fish. Aquat. Sci.* 38, 1385–1392. doi: 10.1139/f81-185

Letelier, R. M., Karl, D. M., Abbott, M. R., and Bidigare, R. R. (2004). Light driven seasonal patterns of chlorophyll and nitrate in the lower euphotic zone of the North Pacific Subtropical Gyre. *Limnol. Oceanogr.* 49, 508–519. doi: 10.4319/lo.2004.49.2.0508

Leu, E., Søreide, J. E., Hessen, D. O., Falk-Petersen, S., and Berge, J. (2011). Consequences of changing sea-ice cover for primary and

secondary producers in the European Arctic shelf seas: timing, quantity, and quality. *Prog. Oceanogr.* 90, 18–32. doi: 10.1016/j.pocean.2011.02.004

Lewis, K. M., Arntsen, A. E., Coupel, P., Joy-Warren, H., Lowry, K. E., Matsuoka, A., et al. (2019). Photoacclimation of Arctic Ocean phytoplankton to shifting light and nutrient limitation. *Limnol. Oceanogr.* 64, 284–301. doi: 10.1002/lno.11039

Lewis, K. M., van Dijken, G. L., and Arrigo, K. R. (2020). Changes in phytoplankton concentration now drive increased Arctic Ocean primary production. *Science* 369, 198–202. doi: 10.1126/science.aay8380

Light, B., Grenfell, T. C., and Perovich, D. K. (2008). Transmission and absorption of solar radiation by Arctic sea ice during the melt season. *J. Geophys. Res.* 113:C03023. doi: 10.1029/2006JC003977

Lind, S., Ingvaldsen, R. B., and Furevik, T. (2018). Arctic warming hotspot in the northern Barents Sea linked to declining sea-ice import. *Nat. Clim. Change* 8, 634–639. doi: 10.1038/s41558-018-0205-y

Lombard, F., Boss, E., Waite, A. M., Vogt, M., Uitz, J., Stemmann, L., et al. (2019). Globally consistent quantitative observations of planktonic ecosystems. *Front. Mar. Sci.* 6:196. doi: 10.3389/fmars.2019.00196

Lovejoy, C., Vincent, W. F., Bonilla, S., Roy, S., Martineau, M. J., Terrado, R., et al. (2007). Distribution, phylogeny, and growth of cold-adapted picoprasinophytes in Arctic seas. *J. Phycol.* 43, 78–89. doi: 10.1111/j.1529-8817.2006.00310.x

Lowry, K. E., Pickart, R. S., Selz, V., Mills, M. M., Pacini, A., Lewis, K. M., et al. (2018). Under-ice phytoplankton blooms inhibited by spring convective mixing in refreezing leads. *J. Geophys. Res. Oceans* 123, 90–109. doi: 10.1002/2016jc012575

Lund-Hansen, L. C., Juul, T., Eskildsen, T. D., Hawes, I., Sorrell, B., Melvad, C., et al. (2018). A low-cost remotely operated vehicle (ROV) with an optical positioning system for under-ice measurements and sampling. *Cold Reg. Sci. Technol.* 151, 148–155. doi: 10.1016/j.coldregions.2018.03.017

Massicotte, P., Bécu, G., Lambert-Girard, S., Leymarie, E., and Babin, M. (2018). Estimating underwater light regime under spatially heterogeneous sea ice in the Arctic. *Appl. Sci.* 8:2693. doi: 10.3390/app8122693

Massicotte, P., Peeken, I., Katlein, C., Flores, H., Huot, Y., Castellani, G., et al. (2019). Sensitivity of phytoplankton primary production estimates to available irradiance under heterogeneous sea ice conditions. *J. Geophys. Res. Oceans* 124, 5436–5450. doi: 10.1029/2019jc015007

Matsuoka, A., Hill, V., Huot, Y., Babin, M., and Bricaud, A. (2011). Seasonal variability in the light absorption properties of western Arctic waters: parameterization of the individual components of absorption for ocean color applications. *J. Geophys. Res. Oceans* 116:C02007.

Matsuoka, A., Larouche, P., Poulin, M., Vincent, W., and Hattori, H. (2009). Phytoplankton community adaptation to changing light levels in the southern Beaufort Sea, Canadian Arctic. *Estuar. Coast. Shelf Sci.* 82, 537–546. doi: 10.1016/j.ecss.2009.02.024

Matthes, L. C., Ehn, J. K., Girard, L.-S., Pogorzelec, N. M., Babin, M., and Mundy, C. J. (2019). Average cosine coefficient and spectral distribution of the light field under sea ice: implications for primary production. *Elem. Sci. Anth.* 7:25. doi: 10.1525/elementa.363

Matthes, L. C., Mundy, C. J., Girard, L.-S., Babin, M., Verin, G., and Ehn, J. K. (2020). Spatial heterogeneity as a key variable influencing spring-summer progression in UVR and PAR transmission through Arctic sea ice. *Front. Mar. Sci.* 7:183. doi: 10.3389/fmars.2020.00183

Mayot, N., Matrai, P., Ellingsen, I. H., Steele, M., Johnson, K., Riser, S. C., et al. (2018). Assessing phytoplankton activities in the seasonal ice zone of the Greenland Sea over an annual cycle. *J. Geophys. Res. Oceans* 123, 8004–8025. doi: 10.1029/2018jc014271

McFarland, C. J., Jakuba, M. V., Suman, S., Kinsey, J. C., and Whitcomb, L. L. (2015). "Toward ice-relative navigation of underwater robotic vehicles under moving sea ice: experimental evaluation in the Arctic sea," in *Proceedings of the 2015 IEEE International Conference on Robotics and Automation (ICRA)*, Seattle, WA, 1527–1534.

McMinn, A., and Martin, A. (2013). Dark survival in a warming world. *Proc. Biol. Sci.* 280:20122909. doi: 10.1098/rspb.2012.2909

Meiners, K. M., Krembs, C., and Gradinger, R. (2008). Exopolymer particles: microbial hotspots of enhanced bacterial activity in Arctic fast ice (Chukchi Sea). *Aquat. Microb. Ecol.* 52, 195–207. doi: 10.3354/ame01214

Michel, C., Hamilton, J., Hansen, E., Barber, D., Reigstad, M., Iacozza, J., et al. (2015). Arctic Ocean outflow shelves in the changing Arctic: a review and perspectives. *Prog. Oceanogr.* 139, 66–88. doi: 10.1016/j.pocean.2015.08.007

Michel, C., Ingram, R. G., and Harris, L. R. (2006). Variability in oceanographic and ecological processes in the Canadian Arctic Archipelago. *Prog. Oceanogr.* 71, 379–401. doi: 10.1016/j.pocean.2006.09.006

Michel, C., Legendre, L., Ingram, R. G., Gosselin, M., and Levasseur, M. (1996). Carbon budget of sea-ice algae in spring: evidence of a significant transfer to zooplankton grazers. *J. Geophys. Res. Oceans* 101, 18345–18360. doi: 10.1029/96jc00045

Michel, C., Legendre, L., Therriault, J.-C., Demers, S., and Vandevelde, T. (1993). Springtime coupling between ice algal and phytoplankton assemblages in southeastern Hudson Bay, Canadian Arctic. *Polar Biol.* 13, 441–449.

Mills, M. M., Brown, Z. W., Lowry, K. E., van Dijken, G. L., Becker, S., Pal, S., et al. (2015). Impacts of low phytoplankton NO3-: PO43- utilization ratios over the Chukchi Shelf, Arctic Ocean. *Deep Sea Res. Part II* 118, 105–121. doi: 10.1016/j.dsr2.2015.02.007

Morel, A., and Bricaud, A. (1981). Theoretical results concerning light absorption in a discrete medium, and application to specific absorption of phytoplankton. *Deep Sea Res. Part A* 28, 1375–1393. doi: 10.1016/0198-0149(81)90039-x

Morel, A., and Gentili, B. (2004). Radiation transport within oceanic (case 1) water. *J. Geophys. Res. Oceans* 109:C06008.

Morin, P.-I., Lacour, T., Grondin, P.-L., Bruyant, F., Ferland, J., Forget, M.-H., et al. (2020). Response of the sea-ice diatom *Fragilariopsis cylindrus* to simulated polar night darkness and return to light. *Limnol. Oceanogr.* 65, 1041–1060. doi: 10.1002/lno.11368

Mundy, C. J., Gosselin, M., Ehn, J., Gratton, Y., Rossnagel, A., Barber, D., et al. (2009). Contribution of under-ice primary production to an ice-edge upwelling phytoplankton bloom in the Canadian Beaufort Sea. *Geophys. Res. Lett.* 36:GL038837. doi: 10.1029/2009GL038837

Mundy, C. J., Gosselin, M., Ehn, J. K., Belzile, C., Poulin, M., Alou, E., et al. (2011). Characteristics of two distinct high-light acclimated algal communities during advanced stages of sea ice melt. *Polar Biol.* 34, 1857–1868.

Mundy, C. J., Gosselin, M., Gratton, Y., Brown, K., Galindo, V., Campbell, K., et al. (2014). Role of environmental factors on phytoplankton bloom initiation under landfast sea ice in Resolute Passage, Canada. *Mar. Ecol. Prog. Ser.* 497, 39–49. doi: 10.3354/meps10587

Nansen, F. (1902). The oceanography of the North Polar Basin. The Norwegian north polar expedition, 1893-1896. *Sci. Res.* 3:427.

Nicolaus, M., and Katlein, C. (2013). Mapping radiation transfer through sea ice using a remotely operated vehicle (ROV). *Cryosphere* 7, 763–777. doi: 10.5194/tc-7-763-2013

Nicolaus, M., Katlein, C., Maslanik, J., and Hendricks, S. (2012). Changes in Arctic sea ice result in increasing light transmittance and absorption. *Geophys. Res. Lett.* 40, 2699–2700. doi: 10.1002/grl.50523

Olsen, L. M., Duarte, P., Peralta-Ferriz, C., Kauko, H. M., Johansson, M., Peeken, I., et al. (2019). A red tide in the pack ice of the Arctic Ocean. *Sci. Rep.* 9:9536.

Oziel, L., Baudena, A., Ardyna, M., Massicotte, P., Randelhoff, A., Sallée, J. B., et al. (2020). Faster Atlantic currents drive poleward expansion of temperate marine species in the Arctic Ocean. *Nat. Commun.* 11:1705.

Oziel, L., Massicotte, P., Randelhoff, A., Ferland, J., Vladoiu, A., Lacour, L., et al. (2019). Environmental factors influencing the seasonal dynamics of under-ice spring blooms in Baffin Bay. *Elem. Sci. Anth.* 7:34. doi: 10.1525/elementa.372

Palmer, M. A., Arrigo, K. R., Mundy, C. J., Ehn, J. K., Gosselin, M., Barber, D. G., et al. (2011). Spatial and temporal variation of photosynthetic parameters in natural phytoplankton assemblages in the Beaufort Sea, Canadian Arctic. *Polar Biol.* 34, 1915–1928. doi: 10.1007/s00300-011-1050-x

Palmer, M. A., Dijken, V. G. L., Mitchell, B. G., Seegers, B. J., Lowry, K. E., Mills, M. M., et al. (2013). Light and nutrient control of photosynthesis in natural phytoplankton populations from the Chukchi and Beaufort seas, Arctic Ocean. *Limnol. Oceanogr.* 58, 2185–2205. doi: 10.4319/lo.2013.58.6.2185

Palmer, M. A., Saenz, B. T., and Arrigo, K. R. (2014). Impacts of sea ice retreat, thinning, and melt-pond proliferation on the summer phytoplankton bloom in the Chukchi Sea, Arctic Ocean. *Deep Sea Res. Part II* 105, 85–104. doi: 10.1016/j.dsr2.2014.03.016

Pavlov, A. K., Taskjelle, T., Kauko, H. M., Hamre, B., Stephen, H. R., Assmy, P., et al. (2017). Altered inherent optical properties and estimates of the underwater light

field during an Arctic under-ice bloom of *Phaeocystis pouchetii*. *J. Geophys. Res. Oceans* 122, 4939–4961. doi: 10.1002/2016jc012471

Perovich, D. K. (2005). On the aggregate-scale partitioning of solar radiation in Arctic sea ice during the Surface Heat Budget of the Arctic Ocean (SHEBA) field experiment. *J. Geophys. Res. Oceans* 110:C03002.

Perovich, D. K., Light, B., Eicken, H., Jones, K. F., Runciman, K., and Nghiem, S. V. (2007). Increasing solar heating of the Arctic Ocean and adjacent seas, 1979–2005: attribution and role in the ice-albedo feedback. *Geophys. Res. Lett.* 34:L19505.

Perovich, D. K., and Polashenski, C. (2012). Albedo evolution of seasonal Arctic sea ice. *Geophys. Res. Lett.* 39:L08501.

Pickart, R. S., Moore, G. W. K., Torres, D. J., Fratantoni, P. S., Goldsmith, R. A., and Yang, J. (2009). Upwelling on the continental slope of the Alaskan Beaufort Sea: storms, ice, and oceanographic response. *J. Geophys. Res.* 114:C00A13.

Pickart, R. S., Spall, M. A., and Mathis, J. T. (2013). Dynamics of upwelling in the Alaskan Beaufort Sea and associated shelf–basin fluxes. *Deep Sea Res. Part I* 76, 35–51. doi: 10.1016/j.dsr.2013.01.007

Polyakov, I. V., Pnyushkov, A. V., Alkire, M. B., Ashik, I. M., Baumann, T. M., Carmack, E. C., et al. (2017). Greater role for Atlantic inflows on sea-ice loss in the Eurasian Basin of the Arctic Ocean. *Science* 356, 285–291. doi: 10.1126/science.aai8204

Proshutinsky, A., Krishfield, R., Toole, J. M., Timmermans, M.-L., Williams, W., Zimmermann, S., et al. (2019). Analysis of the Beaufort Gyre freshwater content in 2003–2018. *J. Geophys. Res. Oceans* 124, 9658–9689. doi: 10.1029/2019jc015281

Randelhoff, A., Lacour, L., Marec, C., Leymarie, E., Lagunas, J., Xing, X., et al. (2020). Arctic mid-winter phytoplankton growth revealed by autonomous profilers. *Sci. Adv.* 6:eabc2678. doi: 10.1126/sciadv.abc2678

Randelhoff, A., Oziel, L., Massicotte, P., Bécu, G., Galí, M., Lacour, L., et al. (2019). The evolution of light and vertical mixing across a phytoplankton ice-edge bloom. *Elem. Sci. Anth.* 7:20. doi: 10.1525/elementa.357

Randelhoff, A., Reigstad, M., Chierici, M., Sundfjord, A., Ivanov, V., Cape, M., et al. (2018). Seasonality of the physical and biogeochemical hydrography in the inflow to the Arctic Ocean through Fram Strait. *Front. Mar. Sci.* 5:224. doi: 10.3389/fmars.2018.00224

Randelhoff, A., and Sundfjord, A. (2018). Short commentary on marine productivity at Arctic shelf breaks: upwelling, advection and vertical mixing. *Ocean Sci.* 14, 293–300. doi: 10.5194/os-14-293-2018

Redfield, A. C., Ketchum, B. H., and Richards, F. A. (1963). "The influence of organisms on the composition of the sea water," in *The Sea*, Vol. 2, ed. M. N. Hill (New York, NY: Interscience Publishers), 26–77.

Regan, H. C., Lique, C., and Armitage, T. W. K. (2019). The Beaufort Gyre extent, shape, and location between 2003 and 2014 from satellite observations. *J. Geophys. Res. Oceans* 124, 844–862. doi: 10.1029/2018jc014379

Rey, F. (2012). Declining silicate concentrations in the Norwegian and Barents Seas. *ICES J. Mar. Sci.* 69, 208–212. doi: 10.1093/icesjms/fss007

Riebesell, U., Schloss, I., and Smetacek, V. (1991). Aggregation of algae released from melting sea ice: implications for seeding and sedimentation. *Polar Biol.* 11, 239–248.

Riedel, A., Michel, C., and Gosselin, M. (2006). Seasonal study of sea-ice exopolymeric substances on the Mackenzie shelf: implications for transport of sea-ice bacteria and algae. *Aquat. Microb. Ecol.* 45, 195–206. doi: 10.3354/ame045195

Rinke, A., Maturilli, M., Graham, R. M., Matthes, H., Handorf, D., Cohen, L., et al. (2017). Extreme cyclone events in the Arctic: wintertime variability and trends. *Environ. Res. Lett.* 12:094006. doi: 10.1088/1748-9326/aa7def

Roemmich, D., Alford, M. H., Claustre, H., Johnson, K. S., King, B., Moum, J., et al. (2019). On the future of argo: a global, full-depth, multi-disciplinary array. *Front. Mar. Sci.* 6:439. doi: 10.3389/fmars.2019.00439

Sakshaug, E. (2004). *Primary and Secondary Production in the Arctic Seas*. Berlin: Springer, 57–81.

Sansoulet, J., Pangrazi, J.-J., Sardet, N., Mirshak, S., Fayad, G., Bourgain, P., et al. (2019). Green edge outreach project: a large-scale public and educational initiative. *Polar Rec.* 55, 227–234. doi: 10.1017/s0032247419000123

Schulze, L. M., and Pickart, R. S. (2012). Seasonal variation of upwelling in the Alaskan Beaufort Sea: impact of sea ice cover. *J. Geophys. Res.* 117:C06022.

Selz, V., Laney, S., Arnsten, A. E., Lewis, K. M., Lowry, K. E., Joy-Warren, H. L., et al. (2018). Ice algal communities in the Chukchi and Beaufort Seas in spring and early summer: composition, distribution, and coupling with phytoplankton assemblages. *Limnol. Oceanogr.* 63, 1109–1133. doi: 10.1002/lno.10757

Sherr, E. B., Sherr, B. F., Wheeler, P. A., and Thompson, K. (2003). Temporal and spatial variation in stocks of autotrophic and heterotrophic microbes in the upper water column of the central Arctic Ocean. *Deep Sea Res. Part. I* 50, 557–571. doi: 10.1016/s0967-0637(03)00031-1

Shirshov, P. P. (1944). *Scientific Results of the Drift Station North Pole*. Russia: USSR Academy of Sciences, Obshchee sobranie, 110–140.

Smith, G. C., Allard, R., Babin, M., Bertino, L., Chevallier, M., Corlett, G. K., et al. (2019). Polar ocean observations: a critical gap in the observing system and its effect on environmental predictions from hours to a season. *Front. Mar. Sci.* 6:429. doi: 10.3389/fmars.2019.00429

Søreide, J. E., Falk-Petersen, S., Hegseth, E. N., Hop, H., Carroll, M. L., Hobson, K. A., et al. (2008). Seasonal feeding strategies of Calanus in the high-Arctic Svalbard region. *Deep Sea Res. Part II* 55, 2225–2244. doi: 10.1016/j.dsr2.2008.05.024

Søreide, J. E., Leu, E. V. A., Berge, J., Graeve, M., and Falk-Petersen, S. (2010). Timing of blooms, algal food quality and *Calanus glacialis* reproduction and growth in a changing Arctic. *Glob. Change Biol.* 16, 3154–3163.

Spall, M. A., Pickart, R. S., Brugler, E. T., Moore, G. W. K., Thomas, L., and Arrigo, K. R. (2014). Role of shelfbreak upwelling in the formation of a massive under-ice bloom in the Chukchi Sea. *Deep Sea Res. Part II* 105, 17–29. doi: 10.1016/j.dsr2.2014.03.017

Strass, V. H., and Nöthig, E. M. (1996). Seasonal shifts in ice edge phytoplankton blooms in the Barents Sea related to the water column stability. *Polar Biol.* 16, 409–422. doi: 10.1007/s003000050072

Stroeve, J., and Notz, D. (2018). Changing state of Arctic sea ice across all seasons. *Environ. Res. Lett.* 13:103001. doi: 10.1088/1748-9326/aade56

Sverdrup, H. U. (1929). The waters on the North-Siberian shelf. The Norwegian north polar expedition with the "Maud" 1918-1925. *Sci. Res.* 4:131.

Sverdrup, H. U. (1953). On conditions for the vernal blooming of phytoplankton. *J. Cons. Int. Explor. Mer.* 18, 287–295. doi: 10.1093/icesjms/18.3.287

Tamelander, T., Reigstad, M., Hop, H., Carroll, M. L., and Wassmann, P. (2008). Pelagic and sympagic contribution of organic matter to zooplankton and vertical export in the Barents Sea marginal ice zone. *Deep Sea Res. Part II* 55, 2330–2339. doi: 10.1016/j.dsr2.2008.05.019

Taskjelle, T., Hudson, S. R., Granskog, M. A., and Hamre, B. (2017). Modelling radiative transfer through ponded first-year Arctic sea ice with a plane-parallel model. *Cryosphere* 11, 2137–2148. doi: 10.5194/tc-11-2137-2017

Timmermans, M.-L., and Marshall, J. (2020). Understanding Arctic Ocean circulation: a review of ocean dynamics in a changing climate. *J. Geophys. Res. Oceans* 125:e2018JC014378.

Toole, J. M., Timmermans, M.-L., Perovich, D. K., Krishfield, R. A., Proshutinsky, A., and Richter-Menge, J. A. (2010). Influences of the ocean surface mixed layer and thermohaline stratification on Arctic Sea ice in the central Canada Basin. *J. Geophys. Res. Oceans* 115:C10018.

Tourangeau, S., and Runge, J. A. (1991). Reproduction of *Calanus glacialis* under ice in spring in southeastern Hudson Bay, Canada. *Mar. Biol.* 108, 227–233. doi: 10.1007/bf01344337

Tremblay, J. -É, Bélanger, S., Barber, D. G., Asplin, M., Martin, J., Darnis, G., et al. (2011). Climate forcing multiplies biological productivity in the coastal Arctic Ocean. *Geophys. Res. Lett.* 38:L18604.

Tremblay, J.-É., and Gagnon, J. (2009). "The effects of irradiance and nutrient supply on the productivity of Arctic waters: a perspective on climate change," in *Influence of Climate Change on the Changing Arctic and Sub-Arctic Conditions*, eds. J. C. J. Nihoul and A. G. Kostianoy. (Netherlands: Springer), 73–93.

Tschudi, M., Meier, W. N., Stewart, J. S., Fowler, C., and Maslanik, J. (2019). *EASE-Grid Sea Ice Age, Version 4 . [1984–2018]*. (Boulder, CL: NASA National Snow and Ice Data Center Distributed Active Archive Center). doi: 10.5067/UTAV7490FEPB

Vader, A., Marquardt, M., Meshram, A. R., and Gabrielsen, T. M. (2015). Key Arctic phototrophs are widespread in the polar night. *Polar Biol.* 38, 13–21. doi: 10.1007/s00300-014-1570-2

van de Poll, W., Abdullah, E., Visser, R., Fischer, P., and Buma, A. (2020). Taxon-specific dark survival of diatoms and flagellates affects Arctic phytoplankton

composition during the polar night and early spring. *Limnol. Oceanogr.* 65, 903–914. doi: 10.1002/lno.11355

Vernet, M., Ellingsen, I. H., Seuthe, L., Slagstad, D., Cape, M. R., and Matrai, P. A. (2019). Influence of phytoplankton advection on the productivity along the Atlantic Water Inflow to the Arctic Ocean. *Front. Mar. Sci.* 6:583. doi: 10.3389/fmars.2019.00583

Wallace, L. O., Van Wijk, E. M., Rintoul, S. R., and Hally, B. (2020). Bathymetry-constrained navigation of argo floats under sea ice on the Antarctic continental shelf. *Geophys. Res. Lett.* 47:e2020GL087019.

Wang, Q., Wekerle, C., Wang, X., Danilov, S., Koldunov, N., Sein, D., et al. (2020). Intensification of the Atlantic water supply to the Arctic Ocean through fram strait induced by Arctic sea ice decline. *Geophys. Res. Lett.* 47:e2019GL086682.

Wassmann, P., Reigstad, M., Haug, T., Rudels, B., Carroll, M. L., Hop, H., et al. (2006). Food webs and carbon flux in the Barents Sea. *Prog. Oceanogr.* 71, 232–287. doi: 10.1016/j.pocean.2006.10.003

Wassmann, P., and Slagstad, D. (1993). Seasonal and annual dynamics of particulate carbon flux in the Barents Sea - a model approach. *Polar Biol.* 13, 363–372. doi: 10.1007/bf01681977

Webster, M., Gerland, S., Holland, M., Hunke, E., Kwok, R., Lecomte, O., et al. (2018). Snow in the changing sea-ice systems. *Nat. Clim. Change* 8, 946–953.

Williams, W. J., and Carmack, E. C. (2015). The 'interior' shelves of the Arctic Ocean: physical oceanographic setting, climatology and effects of sea-ice retreat on cross-shelf exchange. *Prog. Oceanogr.* 139, 21–41.

Wollenburg, J. E., Katlein, C., Nehrke, G., Nöthig, E. M., Matthiessen, J., Wolf-Gladrow, D. A., et al. (2018). Ballasting by cryogenic gypsum enhances carbon export in a *Phaeocystis* under-ice bloom. *Sci. Rep.* 8:7703.

Woodgate, R. A. (2018). Increases in the Pacific inflow to the Arctic from 1990 to 2015, and insights into seasonal trends and driving mechanisms from year-round Bering Strait mooring data. *Prog. Oceanogr.* 160, 124–154. doi: 10.1016/j.pocean.2017.12.007

Yager, P. L., Connelly, T. L., Mortazavi, B., Wommack, K. E., Bano, N., Bauer, J. E., et al. (2001). Dynamic bacterial and viral response to an algal bloom at subzero temperatures. *Limnol. Oceanogr.* 46, 790–801. doi: 10.4319/lo.2001.46.4.0790

Zhang, J., Ashjian, C., Campbell, R., Spitz, Y. H., Steele, M., and Hill, V. (2015). The influence of sea ice and snow cover and nutrient availability on the formation of massive under-ice phytoplankton blooms in the Chukchi Sea. *Deep Sea Res. Part II* 118, 122–135. doi: 10.1016/j.dsr2.2015.02.008

Zhang, Q., Gradinger, R., and Spindler, M. (1998). Dark Survival of Marine Microalgae in the High Arctic (Greenland Sea). *Polarforschung* 65, 111–116.

Zhao, M., Timmermans, M.-L., Cole, S., Krishfield, R., Proshutinsky, A., and Toole, J. (2014). Characterizing the eddy field in the Arctic Ocean halocline. *J. Geophys. Res.* 119, 8800–8817. doi: 10.1002/2014jc010488

Zhao, M., Timmermans, M.-L., Cole, S., Krishfield, R., and Toole, J. (2016). Evolution of the eddy field in the Arctic Ocean's Canada Basin, 2005–2015. *Geophys. Res. Lett.* 43, 8106–8108. doi: 10.1002/2016gl069671

Conflict of Interest: The authors declare that the research was conducted in the absence of any commercial or financial relationships that could be construed as a potential conflict of interest.